Master's thesis

The role of thiol-disulfide oxidoreductases on neural stem cell differentiation

to attain the academic degree

Master of Science

in Biochemistry

Department of Neurology

Heinrich-Heine-University

and

University Clinic Düsseldorf

Submitted by:

Samet Kurt

*23.01.1996

Düsseldorf, 11.07.2022

Honorary declaration

I hereby assure, that I have written this master thesis myself and without using any other material, then the cited sources and aids. All posts taken from the sources have been identified as such. The thesis in the same or similar form has not been submitted to any examination body and has not been published.

Düsseldorf, 11.07.2022

Samet Kurt

First examiner: Prof. Dr. rer. nat. Andreas Reichert

Second examiner: PD Dr. rer. nat. Carsten Berndt

Table of contents

1. Abstract

Oxidoreductases plays the vital roles in all aspects of cell biology. Here, we examined the role of Grx2, a glutathione-dependent enzyme catalysing the reversible S-deglutathionylation of various key proteins implicated in cellular metabolism, signal transduction, gene expression and cell motility, in differentiation of neural stem cells and oligodendrocyte progenitors. By using neuronal-OPC co-cultures we show that genetically mediated *Grx2* deletion in NG2+ oligodendroglial lineage leads to substantial decrease in generation of MBP-expressing myelinating cells. Increase in the total number of Olig2+ cells (mature and oligodendrocyte precursors) in mutant cells rules out the cell toxic effect of Grx2 deficiency on lineage survival and may argue for stage specific role of Grx2 required for proper myelin synthesis and, hypothetically, for establishment of myelin sheath. Analysis of mitochondrial activity in $Grx2^{-/-}$ stem/progenitor cells revealed a drastic decrease of mitochondrial membrane potential (MMP). In line with this, supplementation of growth media with recGrx2 enhanced MMP of cultured cells. The later effect was not associated with changes in generation of mitochondrial superoxide under basal conditions or upon NMDA-induced stimulation of NG2+ OPCs, as suggested by measurements with mitosox sensor dye. Results of present study expand our previous observation that *in vitro* differentiation of NG2+ immature OPCs is under control of Grx2 activity. Taking into account that various steps of oligodendroglial differentiation and particularly the synthesis of lipid-rich myelin proteins are primarily dependent from the mitochondrial ATP production as well as mitochondria-generated metabolic intermediates (e.g. carbone bones, acetyl-CoA), these results may point to a novel mechanism by which primary-mitochondria specific oxidoreductase, Grx2, supports energetic and metabolic demands of myelinating cells in the CNS.

2. Introduction

2.1. Redox regulation

Health and disease in ancient medicine were explained by the doctrine of bodily humors (blood, yellow bile, phlegm and black bile). First introduced in the Corpus Hippocraticum (around 400 BCE), disease was described as an imbalance between humors and environment (dyskrasia) which led to phenotypes with specific qualities (hot, cold, dry, moist). Opposing those qualities with dietary changes and secondary metabolites balances the humors and brings health (eukrasia). Humoralism dominated European medicine for almost 2000 year until 1858, when it was disproven by Rudolf Virchow. He introduced cellular pathology, wherein physiochemical disturbances in cells lead to aberrant physiological function (1, 2). Accumulating evidence highlights reduction and oxidation (redox) reactions as the basis of those disturbances (3–6) and suggests redox systems of oxidants, antioxidants and enzymes as an important factor of cellular identity and disease. Oxidative stress, first introduced by Sies and Cadenas in 1985 (7), describes an imbalance between oxidants and antioxidants leading to oxidative damage at lipids, carbohydrates, proteins and DNA thereby leading to damage and death of cells (oxidative distress)(7, 8). In oxidative eustress however, the importance in physiological levels of ROS was linked to redox regulated biological processes like proliferation (9), differentiation (10) and apoptosis (11, 8). ROS are a byproduct of aerobic metabolism and essential for cellular redox signaling. They can improve health and slow down aging (5) while an elevated formation and accumulation lead to various diseases like cancer, diabetes, (neuro)-inflammation and neurodegeneration (12).

Redox signaling depends on reversible posttranslational oxidative thiol modifications regulated by enzymes (6). The amino acid most susceptible to oxidization is cysteine with its thiol (R-SH) residue. Cysteine is underrepresented in all organisms (2.26 % in protein in humans) and its abundancy correlates positively with the complexity of an organism (13). Depending on its pKa value and the local pH level, thiols are subject to deprotonation and formation of thiolate anions ($R\text{-}S^-$). This form is redox sensitive and can be sequentially oxidized to sulfenic, sulfonic and sulfinic acid leading to protein dysfunction. Cysteine based oxidative post translational modifications (PTM) control major developmental programs including stem cell expansion, proliferation, migration and cell fate decision (3). Only a few of surface exposed cysteines are target for redox

modifications and enzymes are needed for PTM including disulfides (RSSR), S-glutathionylation (RSSG) and nitrosylation (RSNO), each of which can shape the metabolic and epigenetic phenotype (14, 15). Cysteines are often crucial for local or global arrangements of an amino acid chain, thereby modulating protein structure, catalysis and function (12). This (in)activation of proteins follows the redox code (16) to form a multilayered and spatiotemporally controlled signaling network, which probably led to complex differentiation processes and the phenotyping of life as we can see it today (3, 5, 17, 18, 6, 4).

Thioredoxins (Trx) were first described as electron donors of ribonucleotide reductase in Escherichia coli (19) but later formed the thioredoxin fold superfamily, key regulators in redox signaling in almost all branches of life (12). Trx catalyzes the reduction of disulfides, nitrosylation and persulfidation and is in return reduced by thioredoxin reductase and nicotinamide adenine dinucleotide phosphate (NADPH) (20). In humans there are several such systems, among others super oxide dismutase (SOD) and peroxiredoxins (Prx), but glutaredoxins are of particular interest.

2.2. Grx 2 maintains cellular thiol redox state

The vertebrate specific GSH dependent oxidoreductase Grx2 maintains cellular thiol homeostasis mainly by catalyzing (de)glutathionylation reactions but can further form/break protein disulfides (figure 1) (21). Grx2 shows enhanced GSH binding and the ability to form iron sulfur clusters. The [2Fe-2S] cluster is coordinated by two active site cysteines and two molecules of non-covalently bound GSH in homo dimeric complexes. (22). Glutathione disulfide (GSSG), one-electron oxidants and reductants can dissociate the cluster and activate Grx2. (23)

The thioredoxin fold ^{37}CSYC^{40} uses both cysteines to reduce disulfides and only the N-terminal cysteine for (de)glutathionylation during a ping pong mechanism (24)(23). In contrast to Trxs, Grx2 has a serine instead of proline in its active site, which gives Grx2 a vaster substrate spectrum, inter alia the formation of iron sulfur clusters and enhanced glutathione binding. Grx2 has two conserved structural cysteines (Cys28 and Cys113) unusual for the Grx family. They form an intra protein disulfide bond to increase the protein stability and its resistance against over oxidation induced inactivation. Oxidated

Grx2 can be reduced by GSH (through GSH reductase (GR) and NADPH) and thioredoxin reductase (through NADPH) (25).

So far there are three known isoforms of Grx2. Grx2a regulates mitochondrial redox homeostasis and protects cells against oxidative stress by preventing caspase-3 and cytochrome c related apoptosis during oxidative stress (26). This isoform was found to be ubiquitously expressed in mitochondria of different tissues (heart, skeletal muscle, kidney, CNS and liver) emphasizing the general importance for mitochondrial redox homeostasis (27). In normal tissue expression of Grx2b and Grx2c was restricted to testes but was additionally found in transcripts of various cancer cell lines. Contrary to Grx2a, the other two isoforms are only found in the nucleus and cytosol probably facilitating cellular differentiation and transformation (27).

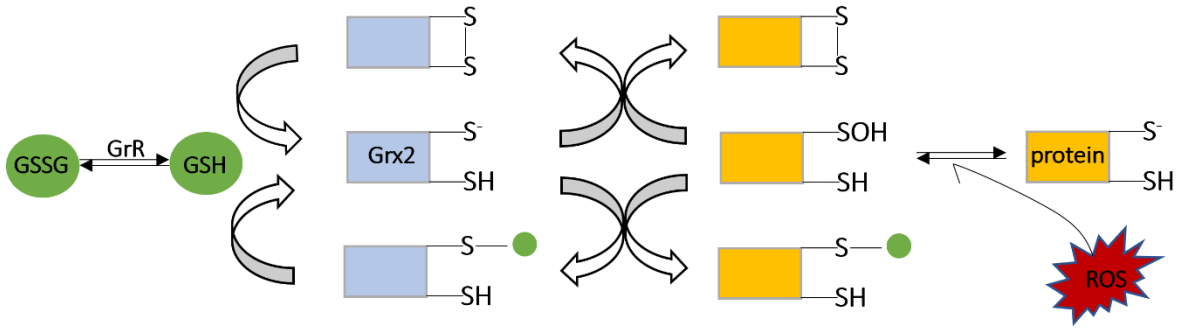

Figure 1: ***Glutaredoxin 2 system***

ROS oxidize protein thiols to sulfenic acid which can form intra- and inter-disulfide bonds. Grx2 catalyzes (de)glutathionylation and disulfide formation/reduction of protein thiols. Oxidative stress favors the formation of sulfenic acid which can form disulfide or be glutathionylated. NADPH+ delivers electrons via glutathione reductase (GR) and GSH to reduce Grx2. Modified from (28)

The oxidizing nature of naturally produced reactive oxygen species (ROS) like superoxide anion (O_2^-), hydrogen peroxide (H_2O_2) or hydroxyl radicals (OH^-) (29) is crucial for redox signaling wherein cysteine thiols act like an on/off switch for proteins . Most of the cellular ROS are derived from NADH:ubiquinone oxidoreductase (complex I) in the electron transfer chain (ETC) (figure 2) (30–33). During aerobic respiration, $NADH^+ + H^+$ is generated through the tricarboxylic cycle (TCA) and delivers two electrons to complex I in the cristae, oxidizing ubiquinone to ubiquinol and fueling the ETC to generate adenosine triphosphate (ATP) at the ATP synthase. 1-2 % of electrons leak during the transport and form ROS. ROS influence epigenetics through oxidation of DNA

methyltransferase (DNMT), histone methyltransferase (HMT) and direct oxidation of nucleotide bases (34). Furthermore they interact with the compartment specific thiol homeostasis (15). Superoxide anions and hydroxyl radicals are more reactive and can directly oxidize DNA, lipids and amino acids. SOD increases the spontaneous transmutation of those molecules into H_2O_2 directly at the site of generation. Catalases can further reduce H_2O_2 to water and high GSH contents protect thiols from irreversible oxidation and cushion electrons from ROS. H_2O_2 is more stable and enhanced in its diffusivity, acting as a redox signaling molecule by oxidizing thiolate anions and GSH. Grx2 is another line in the enzymatic defense which promotes (de)glutathionylation to protect proteins from over oxidization by (in)activating them to initiate transcriptional machineries in response to endogenous and exogenous stimuli. An excess in H_2O_2 forms irreversible modifications at thiolates, nucleotides, carbohydrates and lipids resulting in the initiation of apoptotic signaling pathways. (6)

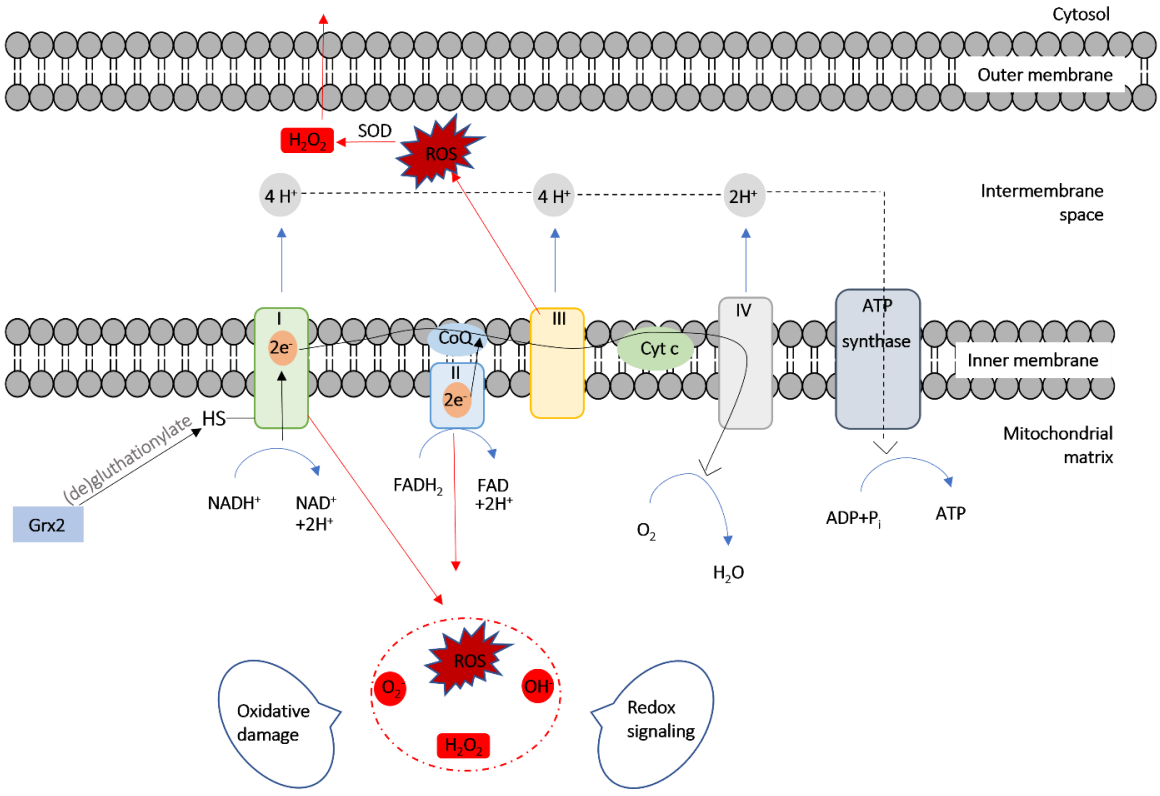

Figure 2: ***Oxidative Phosphorylation***

Mitochondrial electron transfer chain gains electrons through complex I or complex II by reducing NADH or $FADH_2$, respectively. Electrons travel through the complexes, release superoxide anions (release sites are marked with red stars) and reduce O_2 to H_2O at complex IV. During the migration of electron, protons (H^+) are transported into the intermembrane space to fuel the ATP synthase and generate ATP. Grx2 can modulate the activity of the first complex by (de)glutathionylation its cysteine thiol (marked in yellow) and therefore limit ROS, ATP and tricarboxylic cycle (TCA) metabolites. Q=coenzyme Q, C=cytochrome C. Modified from (32)

2.3. Mitochondria and cell identity

Redox homeostasis is predominantly influenced by mitochondrial ROS generation, making them cellular hubs of redox reactions. They prime epigenetics and the cellular phenotype through metabolites, bioenergetics, redox- as well as calcium balance (34). Low mitochondrial respiration is maintained by stem cells, while nutrient availability greatly influences the metabolic phenotype (35, 36). However differentiating cells show an increase in aerobic respiration and ROS generation (34, 37). A decline in mitochondrial function disrupts redox balance with increased ROS production and loss of cellular antioxidant defense, a phenotype observed in aging and disease (38, 37, 17). Mitochondria are essential for cellular processes and redox homeostasis, however mitochondrial dynamics, metabolism and function are redox regulated (39). Redox signaling in mitochondria can promote cell death pathways associated with necrosis, apoptosis and autophagy but also influences mitochondrial bioenergetics (e.g. ATP, ROS production), dynamics (fusion and fission) and metabolic profile (e.g tricarboxylic cycle, beta-oxidation) (6).

An increase in GSSG leads to enzyme mediated oxidation of exposed thiols, making them susceptible for reversible glutathionylation, a reaction catalyzed by Grx2 (21). Small changes in the mitochondrial 2GSH:GSSG pool can already dissociate the iron sulfur cluster of Grx2 and activate downstream signaling (40). Scalcon et. al investigated the thiol regulation of Grx2 in a mitochondrial Grx2 depleted mice model. Abundance and glutathionylation pattern of different mitochondrial enzymes were altered affecting the overall lipid metabolism. (41) Mice showed an altered mitochondrial morphology and functioning with an increase in blood lipid levels. Another group demonstrated that Grx2 regulate mitochondrial structure and autophagy in skeletal muscle cells.(30). In human lens epithelial cells, complex I activity in mitochondria is protected by Grx2 overexpression preventing H_2O_2 induced apoptosis (26), while ROS release from mitochondria is regulated by Grx2 in liver and cardiac cells (32). Thioredoxin reductase inhibition with auranofin or 4-hydroxynonenal leads to excessive amounts of oxidized Trx and subsequently to apoptosis. Cell death was saved by Grx2, acting as a backup to replace functions of Trx1 and 2. (42).

During oxidative stress complex I was shown to be persistently inhibited by glutathionylation via Grx2 (21). A decrease in mitochondrial activity can lead to a change

in the metabolic profile but also prevent further oxidative damage by limiting ROS generation. Low levels in ATP induce AMP-activated kinase (AMPK) and the following activation of histone acetylase and phosphatases, regulating cellular stress-responsive genes and inhibiting cellular growth (34, 43). When redox homeostasis is reached again, Grx2 initiates the deglutathionylation of complex I and upregulates the generation of ATP and ROS (21), influencing the epigenetic landmark.

2.4. Neural stem cell differentiation

Specialization of embryonic and adult neural stem cells (NSC) are accompanied by timely coordinated metabolic profiles including, lipid metabolism, ROS signaling, redox state, glutaminolysis and OXPHOS (44). Human NSC are maintained in hypoxic niches in the subgranular zone (SGZ) of hippocampal dentate gyrus and in the subventricular zone (SVZ) of the lateral ventricles, where low oxygen promotes aerobic glycolysis through the redox mediated stabilization and subsequent activation of hypoxia inducible factor 1α (Hif-1α) (45, 46). This metabolic program supports the maintenance of stemness by providing biomass through glycolysis and suppressing mitochondria to prevent mitochondrial ROS related DNA damage (47–49). NPC can differentiate into neurons and glia cells (45). A tightly regulated epigenome accompanies NSC through five stages of differentiation, namely [1] exit of quiescent, [2] proliferation [3]migration, [4] terminal differentiation, and [5] integration in existing network (31). Transition between stages can be modulated with reversible oxidative PTM to dynamically adapt the epigenome and thus cellular function. Alterations in the redox state are crucial for neural proliferation and differentiation (50).

Grx2 was shown to be essential for brain development. In Zebrafish, silencing of Grx2 lead to apoptotic loss of virtually all neurons as well as the ability to establish an axonal scaffold. Axonal outgrowth, neural survival and development are regulated via the Grx2 mediated reduction of collapsin response mediator protein 2 (CRMP2). (51, 10). Grx2 knock down in zebrafish showed inhibited migration of cardiac neural crest cells, probably through targeting actin and CRMP2 (52). Cell lines expressing Grx2c dramatically changed their morphology, migrated two-fold faster and infiltrated collagen matrix (53). A further target for Grx2c redox modification is the transcription factor SP-1, which enhances the expression of chondroitin sulfate proteoglycan nerve/glial antigen 2

(NG2) increasing NG2 glia population and their migration in vitro, while MBP forming cells were reduced (54).

Mitochondrial dynamics coordinate cell differentiation (55) and are target to thiol modifications, where Grx2 plays a vital role in the modulation of mitochondrial bioenergetics (56). Redox signaling is vastly influenced by mitochondrial ROS, which gradually increase during differentiation (37, 50). As described above, Grx2 can reversibly mediate ROS- and ATP-production through modulation of mitochondrial complex I. ROS signaling modulates major developmental transcription factors including NRF2, NF-kB, AP-1 and Hif-1 (37). For instance nuclear factor erythroid 2-related factor 2 (NRF2) gene expression promotes stress response systems (57) and neural differentiation (50).

2.5. Aims

Grx2 has a variety of targets affecting redox homeostasis and probably the cellular metabolome. Developmental machineries are tightly bound to metabolic programs and Grx2 might be a crucial player in the time dependent coordination of signaling pathways. This work aims to provide tools to investigate processes during neural development/differentiation and to test the hypothesis that Grx2 is a key player in these processes.

In particular, this study will investigate the following three specific points: (I) Establishment of in vitro cultures based on cell lines and human NSCs (derived from iPSCs) and ex vivo cultures based on isolated primary mouse neurons as well as mouse NSCs to study morphological and biochemical changes controlled by Grx2, (II) Analysis of the importance of interaction between NG2 glia and neurons for migration and differentiation of oligodendrocytes/oligodendrocyte progenitor cells using cocultures of primary mouse cells, immunocytochemistry and enzymatic assays, (III) Identification of a Grx2-dependent interplay between mitochondrial activity and neurite outgrowth as well as synaptogenesis.

3. Material and methods

3.1. Materials

3.1.1. Bacterial strains

Below an overview of the bacterial strains I used.

Table 1: Overview of the bacterial strains used

Strain	Genotype	Reference
Escherichia coli BL21(DE3)pLYS	hasdS gal (λIts857 ind 1 Sam7 nin5 lac UV5-T7 gene 1)	Stratagene, USA
XL1-Blue	recA1 endA1 gyrA96 thi-1 hsdR17 supE44 relA1 lac [F´ proAB lacIqZΔM15 Tn10	Stratagene, USA
Clear Coli BL21(DE3)	-	E. M. Hanschmann

3.1.2. Plasmid constructs

The plasmids used in this thesis are listed below

Table 2: Overview of the plasmid constructs used

Name	Vector	Properties	Resistance	Reference
hTrx1	pET-15b	Expression of human Trx1 in bacteria	Ampicillin	C. Berndt
mGrx2c	pET-15b	Expression of murine Grx2 in bacteria	Ampicillin	C. Berndt
mGrx2 C37S	pET-15b	Expression of murine Grx2c C37S in bacteria	Ampicillin	C. Berndt

3.1.3. Antibodies

Primary and secondary antibodies with recommended dilutions are listed in table 3 and 4, respectively.

Table 3: Overview of the primary antibodies and the dilutions used

Host	Target	Dilution	Supplier
Mouse	b-III-Tubulin (Tuj1-clone)	1:200	Sigma-Aldrich, USA
Rat	MBP	1:500	Sigma-Aldrich, USA
Guinea pig	Homer 1	1:500	SYSY, Germany
Mouse	Neurofilament H (SMI-31)	1:1000	Sigma-Aldrich, USA
Rabbit	NG2	1:200	Sigma-Aldrich, USA
Rabbit	Olig2	1:400	Sigma-Aldrich, USA
Rabbit	Synapsin I/II	1:500	SYSY, Germany
Rabbit	Dkk1	1:10000	C. Berndt
Mouse	p53	1:10000	C. Berndt

Table 4: Overview of the secondary antibodies and the dilutions used

Target	Conjugate	Dilution	Supplier
Mouse	Cy2	1:500	Sigma-Aldrich, USA
Rat	Cy3	1:500	Sigma-Aldrich, USA
Rabbit	Cy3	1:500	Sigma-Aldrich, USA
Guinea pig	Cy5	1:500	Sigma-Aldrich, USA
Rabbit	Cy 5	1:500	Sigma-Aldrich, USA
Rabbit	800 nm	1:15000	Sigma-Aldrich, USA
Mouse	680 nm	1:15000	Sigma-Aldrich, USA

3.1.4. Cell culture, media, and supplements

Media and Buffer

1. Dulbecco's Modified Eagle Medium, 4.5g/L D-Glucose, Thermo Fischer Scientific, USA
2. DMEM/F12, Thermo Fischer Scientific, USA
3. DMEM/F12 HEPES, Thermo Fischer Scientific, USA
4. Dulbecco's Phosphate Buffered Saline (DPBS), Thermo Fischer Scientific, USA
5. Hank's Balanced Salt Solution (HBSS), Thermo Fischer Scientific, USA
6. Neurobasal™ Medium, Thermo Fischer Scientific, USA
7. Phosphate Buffered Saline (PBS, pH 7.4), Thermo Fischer Scientific, USA

Cytokines (recombinant)

1. BDNF Protein, CF (human), R&D systems
2. FGF-basic/FGF-2 (mouse), Immunotools
3. EGF (mouse), Immunotools
4. FGF-8a Protein, CF (human), R&D systems
5. GDNF protein (human), R&D systems
6. PDGF-AA (mouse), Immunotools
7. TGF-beta3, ACF (human/mouse), Stemcell Technologies

Supplements

1. B27- Supplement without Vitamin A, Life Technologies, USA
2. B27+ Supplement with Vitamin A, Life Technologies, USA
3. Fetal calf serum (FCS), VWR, Germany
4. Glucose, Thermo Fischer Scientific, USA
5. Glutamine, Thermo Fischer Scientific, USA
6. GlutaMAX, Life Technologies, USA
7. MEM solution out of non-essential amino acids, Thermo Fischer Scientific, USA
8. N-2 Supplement, Thermo Fischer Scientific, USA
9. Pyruvate, Thermo Fischer Scientific, USA

Additives

1. ATP (Adenosine 5‘-triphosphate disodium salt hydrate), Sigma-Aldrich, USA
2. HEPES (4-(2-hydroxyethyl)-1-piperazineethanesulfonic acid), Thermo Fischer Scientific, USA
3. CHIR 99021, Caymen Chemical
4. Dibutyryl cyclic-AMP sodium salt , Merck, Germany
5. Mycokill
6. Penicillin-Streptomycin (P/S), Thermo Fischer Scientific, USA
7. Purmorphamine, MACS Miltenyi, Germany
8. T3 hormone
9. T4 hormone
10. Vitamin C ((+)-Sodium L-ascorbate), Sigma-Aldrich, USA

3.1.5. Chemicals/Proteins

1. Acrylamide/Bis Solution30%, Bio-Rad Laboratories, USA
2. Ampicillin, Thermo Fischer Scientific, USA
3. Ammonium persulfate (APS), Sigma-Aldrich, USA
4. Bovine albumin fraction (BSA), Carl Roth, Germany
5. Calcium chloride, Thermo Fischer Scientific, USA
6. Chloramphenicol, Thermo Fischer Scientific, USA
7. Coomassie Brilliant Blue, Roth, DE
8. 2-Propanol (Isopropanol, Merck, Germany
9. 2,2',2'',2'''- (Ethane-1,2- diyldinitrilo) tetra acetic acid (EDTA), Sigma-Aldrich, USA
10. Dimethyl sulfoxide (DMSO), Merck, Germany
11. Distilled H2O DNase/RNase free, Invitrogen, Germany
12. DNAse I, Merck, Germany
13. EDTA, Life Technologies, USA
14. Ethanol absolute, Merck, Germany
15. Fura-2AM,
16. Glycerol, Sigma-Aldrich, USA
17. Glycine, Sigma-Aldrich, USA
18. Hoechst 33258, Sigma-Aldrich, Germany
19. Hydrochloric acid (HCl), Merck, Germany
20. ImmoMount, Thermo Scientific, USA
21. Isopropyl-β-D-thiogalactopyranosid (IPTG), Roth, DE
22. Kanamycin, Thermo Fischer Scientific, USA
23. LB Agar, Invitrogen, USA
24. LB-Bouillon (Lennox), Invitrogen, USA
25. Luria Broth Base (Miller's LB Broth Base), Invitrogen, USA
26. Matrigel, Sigma-Aldrich, Germany
27. MitoSox red, Invitrogen, USA
28. N-Ethylmaleimide (NEM), Sigma-Aldrich, USA
29. Normal goat serum (NGS), Sigma-Aldrich, Germany
30. Papain 10x, Thermo Fischer Scientific, USA

31. Poly-L-ornithine 0.01% solution, Sigma-Aldrich, USA
32. Ponceau S Solution, Merck, Germany
33. Power SYBR Green Master Mix, Life Technologies, USA
34. Protein Sample SDS Loading Buffer (4X), LI-COR Biosciences, USA
35. Protein-Marker IV, peqGOLD, VWR, Germany
36. RIPA buffer Sigma-Aldrich, Germany
37. Roti-Histofix 4%, Carl Roth, Germany
38. Red Blood Cell Lysis Buffer, Thermo Fischer Scientific, USA
39. Sodium carbonate, Sigma-Aldrich, USA
40. Sodium chloride, Sigma-Aldrich, USA
41. Sodium dodecyl sulfate (SDS), Carl Roth, Germany
42. Sodium hydroxide (NaOH), Sigma-Aldrich, USA
43. StemPro accutase cell dissociation reagent, Thermo Fischer Scientific, USA
44. TEMED (N,N,N',N'-Tetramethylethylenediamine), Sigma-Aldrich, USA
45. Tris-HCl, Carl Roth, Germany
46. Tris-Base, Carl Roth, Germany
47. Tris-Glycine-SDS-buffer, VWR Life Science, USA
48. Triton X-100, Sigma-Aldrich, USA
49. Trypan blue, Thermo Fischer Scientific, USA
50. Trypsin (10x), Life Technologies, USA
51. Tween-20, Sigma-Aldrich, USA

3.1.6. Laboratory Equipment

1. Automated Cell Counter TL10, BioRad, USA
2. BioPhotometer, Eppendorf
3. Centrifuge 5417R, Eppendorf, Germany
4. Centrifuge Rotana 460 R, Hettich, Germany
5. Centrifuge Minispin, Eppendorf, Germany
6. CO2 cell culture incubator, Thermo Scientific, USA
7. F-View CCD Camera, Olympus, Japan
8. Leica TCS SP8 confocal microscope, Leica
9. Mini Protean tetra system, BioRad, USA

10. Nanodrop 2000 Spectrophotometer, Thermo Scientific, USA
11. Odyssey Infrared Imaging System, LI-Cor, USA
12. Olympus BX51, Olympus, Japan
13. Olympus U-RFL-T Burner, Olympus, Japan
14. pH-Meter, HANNA Instruments, USA
15. Pipettes, Eppendorf, Germany
16. TECAN GENios Microplate Reader, Tecan Group LTD, Switzerland
17. Thermocycler T Gradient, Biometra, Germany
18. Trans-Blot Turbo transfer system, BioRad, USA
19. Vortex Genie2, Scientific Industries, USA

3.1.7. Software

1. ChemDraw Professional 16, PerkinElmer Informatics
2. Citavi 6, Swiss Academic Software
3. Fiji, Wayne Rasband
4. GraphPad Prism5, PraphPad Software Inc.
5. ImageJ, Wayne Rasband
6. LASX image acquisition, Leica
7. MS Office 365, Microsoft Corporation
8. Odyssey Imaging System Software, LI-COR

3.2. Methods

3.2.1. Recombinant expression of human Grx2c

3.2.1.1. Chemical competent cells

BL21(DE3) pRIL competent bacteria were plated on LB-agar plates (+100 µL ampicillin) and incubated overnight (37 °C, shaking). One colony was transferred to 10 mL LB medium (overnight,37 °C, shaking). 6 ml were then diluted in 100 mL LB-medium (+100 µL ampicillin). Bacteria were grown at 37 °C (shaking) until an OD_{600} of 0,6 was reached. Culture was then incubated at 4 °C, centrifuged (11000 g, 15 min) and resuspended in 33 mL 0,1 M $CaCl_2$. After 15 min incubation at 4 °C, cells were again centrifuged and the supernatant was discarded. Pellet was resuspended in 4 mL 0,1 M $CaCl_2$ +15 % glycerol

and incubated at 4 °C for 15 min. Then 200 µL aliquots were prepared and stored at -80 °C.

3.2.1.2. Transformation

0.3 µL of plasmid (concentration 50-100 ng/µL) were added to 200 µL BL21(DE3) pRIL or XL1-Blue bacteria and incubated on ice for 3 min. After a 1 min heat shock at 42 °C, cells were transferred on ice again for 2 min. 500 µL LB-medium was added and incubated for 45 min (37 °C, 150 rpm). Then, 100 µL of cell suspension was plated out on an agar plates supplemented with 100 µg/ml ampicillin (BL21(DE3) pRIL) or 50 µL kanamycin/100 µL ampicillin (XL1-Blue).
Clear coli bacteria were already transformed with appropriate plasmid and provided by Kathrin Brücksken who got them from E. M. Hanschmann.

3.2.1.3. Plasmid isolation

One colony of freshly transformed XL1-Blue bacteria was incubated in 10 mL LB-medium (50 µL kanamycin/100 µL ampicillin) overnight at 37 °C shaking. Plasmid was isolated from 10 mL culture with the Miniprep kit (Promega) as described by the manufacturer. Sequencing was conducted via SeqLab and sequence was controlled online with the Swiss Bioinformatics Resource Portal Expasy.

3.2.1.4. Overexpression

The Grx2c-expressing plasmid was amplified in XL1-blue strain, isolated and sequenced. Sequencing showed no mutations and the plasmid was transformed in newly produced chemically competent BL21(DE3)pLYS *E. coli*. Plasmids (see materials 3.1.2) encoding mouse Grx2c, mutant mouse Grx2 C37S (Grx2-trap) and human Trx1 were transformed in ClearColi strain or competent *E. coli* cells and plated out. Single colony was picked from a fresh transformation and transferred to 10 mL of LB medium (100 µL ampicillin) in a 50 mL falcon. The overnight culture was incubated at 37 °C shaking. The next day, 100 µL were transferred to two new falcons with 10 mL LB-medium and incubated until an OD_{600} of 0.6 was reached at 37 °C shaking. One culture was then induced with 1 µM Isopropyl β-D-1-thiogalactopyranoside (IPTG) and both were incubated over night at room temperature shaking. An OD_{600} of 1 was removed and centrifuged at full speed for 5 min.

Pellets were resuspended in 50 µL 1x protein sample SDS loading buffer, incubated at 95 °C, centrifuged and repeated until no pellet formed anymore. 35 µL were loaded on 16 % polyacrylamide gel and analyzed via SDS PAGE. It is expected, that Grx2/Trx1 overexpressing cultures show a thick band with MW around 16 and/or 32 kDa in the IPTG-induced lysates. Note: for further experiments recombinant hGrx2c was provided by the lab of Christopher Horst Lillig from the University of Greifswald.

3.2.2. Cell culture

All work with cells was performed under a sterile bench. Cells were cultivated in a humidified incubator with 37 °C and 5 % CO_2. Half of medium was exchanged every 2 days and whole medium at every third exchange.

3.2.2.1. Splitting and passaging cells

Adherent cells were collected when confluency was reached, either by scraping, splashing, trypsinization or with accutase depending on the cell type. For this, the medium was removed beforehand and cells were washed once with PBS. Cells were then centrifuged at 200 g for 5 min, resuspended in 1 ml medium and singularized mechanically by pipetting up and down. The suspension was then split in a ratio up to 1:10 and seeded in a new dish with fresh medium. For assays, cells were counted before seeding via a cellcounter by mixing 10 µL of the 1 mL cell suspension with 10 µL Trypan blue. Cells were usually split once every 3-5 days.

3.2.2.2. Freezing cells

Cells were frozen in 20 % DMSO. For this, cells were resuspended in 800 µL media and kept on ice for 5 min in cryo nuncs. 800 µL media containing 40 %DMSO was then added drop wise on the cells, inverted once and placed in a cryo box with isopropanol. Box was then stored at -80 °C overnight. The next day nuncs were transferred into normal plastic boxes at -80 °C.

3.2.2.3. Thawing cells

PBS with 10 % media was prewarmed at 37 °C in a 15 mL falcon. Prewarmed buffer was added to the cryo nunc with frozen cells, pipetted up and down and mixed back into the

falcon. This process was repeated until whole batch was thawed and diluted in buffer. The falcon tube was then centrifuged at 200 xg for 5 min, pellet was resuspend in 1 mL of appropriate media and seeded for further use.

3.2.2.4. Coating dishes

For most cells, 13 mm cover glasses and dishes were coated with 0,1 mg/mL ploy(L)-lysin. Coating solution diluted in PBS was added into the dish and incubated over night at 37 °C. Dishes were then washed 3 times with PBS before seeding cells.

Frozen Matrigel was diluted in cold DMEM to 5 mg/mL on ice. The solution was then aliquoted and stored at -20 °C until further use. For coating, aliquots were further diluted to 200 µg/mL in DMEM, added to cover glasses/dishes and incubated over night at 4 °C. Before use, glasses/dishes were pre-warmed at 37 °C and washed once with PBS.

3.2.2.5. Conditional media

Glial cells were grown on Poly-O coated dishes in Neurobasal medium (supplemented with 1 % GlutaMax, 1 % Pen/Strep, B27+ 1:50, 10 % FCS). After one week medium was discarded and the same medium without FCS was added. After 4 days, medium was collected, stored at –20 °C and used as conditional media. The process was repeated until cells changed morphology or died. This media contains secreted molecules which are needed for the growth and differentiation of neuronal cells.

3.2.3. Isolation, maintenance and differentiation of cells

3.2.3.1. NSPC culture

Neuronal stem and progenitor cells (NSPC) were isolated as Guo et al (58) described before. Mice (up to five days old) were sacrificed, disinfected in 70% Ethanol, and decapitated above the cervical spinal cord. Brains were spatulated out the opened skull and meninges was removed. It was then placed in $HBSS^-$ over ice. Dentate gyrus (DT) and subventricular zone (SVZ), containing NSPCs, were obtained by chopping the whole brain in slices with a chopper and dissecting them under a binocular. Desired tissue was collected in $HBSS^-$, centrifuged at 200 xg for 5 min and aspirated. Pre-warmed papain in DMEM/F12 was supplemented with DNase (50 u/mL) and added to the pellet. Covered tissue was incubated up to 30 min at 37 °C and triturated with a pipette every few minutes

until a homogeneous suspension formed. Next the suspension was filtered through a 40 µm nylon mesh to remove myelin and debris, diluted with HBSS (-) and centrifugated. The pellet was resuspended in erythrocytes lysis buffer and incubated for 3 min at 4 °C. After incubation, the falcon was filled with PBS and centrifuged at 200 xg for 5 min. Supernatant was aspirated and the pellet, containing a mix of cells, was resuspended in neurobasal medium (1 % GlutaMax, 1 % Pen/Strep, B27- 1:50, bFGF and EGF (20 ng/ml)) and seeded into 10 cm culture dishes. Cell mixture was incubated for 4 days at 37 °C (5% CO_2), while bFGF and EGF were supplemented again after 2 days. Then, medium containing floating neurospheres was collected and attached glial cells were refreshed with new media and kept for later conditional media production. Neurospheres were centrifuged at 200 g for 5 min and singularized with accutase for 5 min while pipetting. After digestion, tube was filled up with PBS centrifuged again and resuspended in 1 mL neurobasal medium (1 % GlutaMax, 1 % Pen/Strep, B27- 1:50, bFGF and EGF (20 ng/ml)). Cells were aliquoted in 1 x 10^6 cells per 1,6 mL medium with 20 % DMSO and stored at -80 °C until further use.
Before differentiation to neurons, NSPCs were seeded on dishes or cover glasses and incubated over nigh in neurobasal medium (1 % GlutaMax, 1 % Pen/Strep, B27- 1:50, bFGF and EGF (10 ng/ml)). The next day media was changed to neurobasal medium (1 % GlutaMax, 1 % Pen/Strep, $B27^+$ 1:50). Cells were then maintained that way up to one month.

3.2.3.2. Neuronal culture

Neurons were isolated from whole mouse brains using the Neural Isolation kit (Miltenyi) according to the manufacturer's instructions. As described for NPCS (without isolating DT and SVZ), brains were collected and cut in small pieces, digested with papain, erythrocytes were lysed with erythrocytes lysis buffer and the pellet was resuspended in sorting buffer ($HBSS^-$ supplemented with 2 g/L glucose, 1 mM pyruvate and 1:100 NEA). Non neuronal cell biotin-antibody cocktail (on magnetic beads) were added to the cell solution and incubated at 4 °C. The suspension was loaded on a column for magnetic cell sorting and washed three times with sorting buffer. Neurons could be found in the flowthrough and washing elution. Those were centrifuged at 200 xg for 5 min, resuspended in Neurobasal medium (with 1% GlutaMax, 1 % Pen/Strep, B27- 1:50, 30 % conditional media) diluted to 4x10^4 cell per 50 µL and seeded drop wise on coated cover glasses. After one day of

regeneration, media was changed to differentiating conditions (Neurobasal medium with 1% GlutaMax, 1 % Pen/Strep, B27$^+$ 1:50, 30 % conditional media).
Bound neural cells were eluted with sorting buffer by removing the column from the magnet and either used for oligodendrocyte precursor cells (OPC) sorting or for generation of conditional media.

3.2.3.3. OPC culture

Sorting of OPCs was performed as described for neurons with the same kit, using different magnetic beads label with antigens for cellmarker proteins. Anti-An2, Anti-NG2 or Anti-O4 beads were used for the isolation of appropriate cell populations. Collected cells were resuspended in OPC proliferation media (DMEM/F12 containing 1% GlutaMax, 1 % Pen/Strep, B27$^-$ 1:50, bFGF and PDGF (20 ng/mL)). For proliferation, cells were seeded on uncoated dishes, while assays and differentiation needed poly(L)-Lysin coated surfaces. Differentiation was initiated with DMEM/F12 containing 1% GlutaMax, 1 % Pen/Strep, B27$^+$ 1:50, T3 and T4.

3.2.3.4. smNPC culture

For the study of human neurons, small molecule neuronal progenitor cells (smNPC) were provided by the lab of Univ.-Prof. Dr. Alessandro Prigione. Patient somatic cells were reprogrammed to induced pluripotent stem cells (iPSC) which were then differentiated to smNPC by them as described in Prigione et al (59) with small molecules.
Maintenance and differentiation of smNPC was achieved with different sets of small molecule cocktails. Frozen aliquots of smNPC were thawed and seeded on Matrigel coated 6-well plate. The base medium (bm-) consisting of DMEM/F12:neurobasal 1:1, N-2 1:100, B27$^-$ 1:100, 1% Pen/Strep, 2 mM glutamine and Mycokill. For proliferation 3µM CHIR, 500 nm purmorphamine and 150 µM Vitamin C were added, while differentiation to dopaminergic neurons need different cocktails at different time points.
Differentiation was initiated with bm+ (plus retinoic acid) containing 100 ng/mL FGF8, 1 µM purmorphamine and 200 µM Vitamin C. After 7 days media was changed to bm supplemented with 10 ng/mL BDNF, 10 ng/mL GDNF, 1ng/mL TGF-b3, 200 µM Vitamin C, 500 µM db c-AMP and 0,5 µM purmorphamine. Then after 2 days bm+ with 10 ng/mL

BDNF, 10 ng/mL GDNF, 1ng/ml TGF-b3, 200 µM Vitamin C and 500 µM db c-AMP was used.

3.2.3.5. Cell lines

Cryo preserved cells were thawed and seeded in DMEM (+ 10 % FCS) for proliferation. Poly-O coated dishes and DMEM (+ 1 % FCS) were used for differentiation. Cells were split using trypsin.

OLN-93 cells resemble primary oligodendrocytes in their antigenic properties and are derived from spontaneously transformed cells in primary rat brain glial cultures. (60). Cryo preserved aliquot was provided by Tim Prozorovski, expanded and new stocks were prepared. Maintenance is described above.

Mouse embryonic fibroblasts (MEF) were provided by Leonie Thewes and maintained as described above.

SN4741 is a retrovirally immortalized cell line of substantia nigra (SN) dopaminergic neurons. They are in a late stage of neuronal progenitor cells (NPCs), already primed to be dopaminergic neurons, and they maintain proliferation at 33 °C in DMEM (+10 % FCS). Differentiation is induced temperature dependent at 39 °C in DMEM (+1% FCS). (61) Cells were provided by Carsten Berndt, expanded and new stocks were prepared.

3.2.4. Immunocytochemistry (ICC)

Coated glasses with grown cells were fixed with 4 % Roti-Histofix for 15 min, shaking at room temperature (RT). After two washing steps with HBSS, cells were permeabilized and blocked for 1 h in blocking buffer (PBS, 0,1 % Triton-X 100, 5 % NGS) to avoid unspecific binding. Primary antibodies were added in appropriate concentration and cells were incubated at 4°C overnight. After washing three times with PBS, secondary antibodies (Cyanine Dyes) and Hoechst diluted in blocking buffer were added for 1 h at RT. Glasses were washed three times with PBS for 10 min and attached to object slides with ImmuMount (Thermo Fisher, USA). Object slides were dried overnight in the dark and pictures were taken using BX51 fluorescent microscope (Olympus, Japan) and F-view CCD camera (Olympus, Japan) or the Lecia TCS SP8 confocal microscope..

A second protocol was later used as described by Ippolito et. al. (62). The procedure was the same but different buffers were used. Antibody buffer was prepared with 150 mM

NaCl, 50 mM Tris-Base and 1% BSA in water. Cells were permeabilize with blocking buffer (50 % antibody buffer, 50 % NGS, 0,2 % Triton-X) for 30 min at RT and antibodies were incubated in antibody buffer (+ 10% NGS).

3.2.5. SDS-PAGE

Sodium dodecylsulfate polyacrylamide gel electrophoresis (SDS-PAGE) was performed to separate proteins by there mass. Either precast gels with a gradient (8- 12 %) or selfmade16 % polyacrylamide gels as described elsewhere (63) were used. Gel electrophoresis was conducted with the MINI-Protein Tetra System from BioRad Laboratories at 140 V for 14 h and using the peqGOLD protein marker IV. Whole proteins were detected by staining gels with Coomassie solution (10 % acetic acid, 40 % ethanol, 0.1 % Coomassie Brilliant Blue), washing overnight in water and the following image acquisition with LI-COR Odyssey Infrared Imaging System.

3.2.6. Western Blot

Proteins from SDS-PAGE gel were transferred to nitrocellulose membrane with the Trans-Blot Turbo Transfer System (BioRad) for 10 min at 1.3 A and 25 V. Membranes were stained with Ponseau to check protein bands and then washed with PBS-T (phosphate buffered saline with 0.5 % Tween-20). After blocking for 1 h in PBS-T with 5 % BSA, membranes were washed once for 10 min with PBS-T and the gel was covered with primary antibody in TBS-T with 2,5 % BSA and incubated over night at 4 °C. Membranes were washed three times a 10 min and the secondary antibody in 2,5 % BSA PBS-T was added for 1 h shaking at room temperature. Then again it was washed three times a 10 min. Image acquisition was performed with LI-COR Odyssey Infrared Imaging System.

3.2.7. Fluorometric assays

Those Assays were conducted with a plate reader in black 96 well plates. The procedure for the different assays were similar. First 2x10^5 cells were seeded in black 96 well plate and incubated over night at 37 °C. On the assay day, medium was exchanged to assay buffer (HBSS-, Penicillin/Streptomycin, 2 g/L glycose, 1 mM pyruvate, 1:100 MEM) and incubated for 30 min at 37 °C.

3.2.7.1. MitoID

Mitochondrial membrane potential (MMP) was measured with the MitoID Membrane potential cytotoxicity kit from Enzo (ENZ-51019). Its cationic dye fluorescence either in green (535 nm) or in orange (590 nm), depending upon MMP. Recovered cells were incubated for 30 min in 100 µL assay buffer at 37 °C and then filled 1:1with prepared dye solution. After another 30 min of incubation at 37 °C, 2-4 µM carbonyl cyanide 3-chlorophenylhydrazone (CCCP) was added as a positive control. CCCP is a proton ionophore and uncoupler of oxidative phosphorylation. Treatment with CCCP leads to depolarization of the MMP. After 15 min of CCCP incubation at 37 °C the fluorescence emission of samples, background (assay buffer + dye solution) and positive control were measured with TECAN plate reader in two channels. Emission at 535 nm (excitation 485 nm) and at 590 nm (excitation 535 nm) were measured twice in 3x3 points per well with the TECAN reader.

3.2.7.2. Ca2+ Assay

Fura-2AM was used to determine intracellular calcium concentrations. Fura-2 can bind acetoxmethylester (AM) and diffuse inside the cell, where esterases digest the AM and activate Fura2. Ca^{2+} saturated Fura2 can be excited at 340 nm and unsaturated at 380 nm while both emit at 510 nm. The ratios 510/340 nm and 510/380 nm directly relate to the intracellular amount of Ca^{2+} (64). Recovered NG2 cells were incubated in assay buffer with 6 µM Fura-2AM and 10 mM Hepes for 45 min at 37 °C. Wells were washed twice with assay buffer and resuspended in assay buffer. Control groups were treated with 0,8 mM GSH and another group with 0,8 mM GSH + 2 µM hGrx2c. Emission was measured with the TECAN reader directly after treatment and 20 min later. Groups were then treated with 40 µM NMDA, 100 µM glutamate or 10 µM kainite. Emission was again measured directly after treatment and 20 minutes later. 26 µM ionomycin was added and measured (needed for calculation of Ca^{2+} concentration). Intensity ratios after blank subtraction were related to intracellular Ca^{2+} concentration with the following equation:

$$[Ca^{2+}] = K_d Q \left(\frac{R - R_{\min}}{R_{max} - R}\right)$$

R represents the fluorescence intensity ratio $F_{\lambda 1}$/ $F_{\lambda 2}$ (λ_1=340 nm and λ_2=380 nm), Q is the ratio of F_{min}(ion free fluorescence) to F_{max} (ion saturated fluorescence)) at 380 nm and K_d the dissociation constant of the indicator. (65)

3.2.7.3. Mitosox Assay

Mitosox assay was conducted in the same way as Ca^{2+} assay. Here 2.5 µM of mitosox dye was used instead of Fura-2AM and fluorescence was measured at 580 nm (excitation 510 nm).

3.2.8. Indirect redox shift

Oxidation status of cysteines were determined with an indirect redox shift (66). 6 wells of SN4741 cells were seeded at 50 % confluency (around 1 million cells), recovered overnight and treated with 1mM LiCl to activate the Wnt signaling for 6 hours. One group was further treated with 2 µM Grx2c. Afterwards, each well was prepared differently (unmodified, minimum shift, maximum shift, steady state control, steady state treat). The plate was put on an ice-cold metal plate and medium of steady state groups (representing the physiological redox state) were removed. Cells were washed with 1mL ice-cold PBS and incubated with 1 mL PBS-NEM (20 mM) to block all accessible Sulfhydrylgroups for 10 min on ice. Meanwhile media from the other samples was removed and cells were washed with PBS. 500 µL of 8 % TCA was added to lyse cells. After the 10 min incubation, cells from all groups were scratched using a cell scraper, transferred into to an 1,5 ml tube and incubated for 1 h at -20 °C. Samples were thawed at room temperature and centrifuged (4 °C, 15min, 13000 g) to precipitate denatured proteins. Supernatant was removed and samples were centrifuged again for 1 min to remove remaining TCA. 50 µL Laemmli buffer (2 % (w/v) SDS, 60 mM Tris-HCl pH 6.8, 10 % (v/v) glycerol, 0.0025 % (w/v) bromophenolblue) + 2 % (w/v) TCEP to untreated group and 46 µL to the remaining groups to reduce all free thiols. pH was adjusted until samples' color turned blue (from yellow). All samples were sonicated at room temperature (10 stroke, 50 % intensity) and incubated for 15 min at 45 °C. After cooling samples at room temperature for 5 min, the minimal shift group was treated with 4 µL 250 mM NEM and remaining groups but the untreated were modified with 4 µL 250 mmPEG (binding reduced thiols to

shift the isoelectric point of the protein). Then samples were incubated for 1 h at RT and analyzed via SDS-PAGE and Wester Blotting.

3.2.9. ATP-Assay

ATP concentrations were measured with a luciferase kit. $1x10^5$ OLN-93 cells per well were seeded in a 6-well-plate and recovered over night at 37 °C. One group was treated with 10 mM 2-desoxy-glucose to inhibit glycolysis (positive control) and another with 40 µM NMDA for one hour. Media was then removed and cells were frozen for one hour at -20 °C and resuspended in 500 µL 5mM TCA. After 5 min, 100 µL were first diluted 3:1 in 20 mM Tris buffer (pH 7.5) and 1:30 in water. A black 96 well plate was loaded with 1:1 sample and luciferase as described by the manufactured and measured with the TECAN reader.

3.2.10. Data Analysis

Images acquired from immunodetection were processed (Background subtraction, unsharp mask filter, noise despeckle) with Fiji and prepared with PowerPoint.

Neurite outgrowth was quantified by measuring the pixel length of β-III-tubullin immunostaining by using NeuroanatomyJ software and its feature Simple Neurite Tracker (SNT), a plug-in for Fiji.

Statistical analysis and plots were performed with GraphPad Prism 5. Significance is indicated with stars (ns $P>0.05$; * $P<0.05$; ** $P<0.01$; *** $P<0.0001$) and calculated with t-test.

4. Results

4.1. Establishment of culture method to evaluate the role of Grx2 in OPC differentiation and OL-neuron contact formation

Previously we demonstrated that Grx2 promotes axonal outgrowth via redox modulation of collapsin response mediator protein 2 (CRMP2) (51, 10), a central component of the semaphorin pathway implicated in neuron migration, repulsive axon guidance and synapse formation (67). CRMP2 is involved in oligodendrocyte (OL) process retraction and oligodendrocyte progenitor cell (OPC) migration and directionality (68). Therefore, we hypothesized that cytosolic Grx2c may contribute to OPC development by regulating cell migration and cell contact formation. In support of this hypothesis we have previously found that differentiating OPCs treated with recombinant Grx2c characterized by enhancement of NG2 and inhibition of myelin basic protein (MBP) expression (54). The later, may point to the role of Grx2 in the long-term maintenance of undifferentiated state of OPCs and promoting the formation of correct contacts with their neuronal targets.

Shape and stage-specific antigen (marker) expression in OPCs change sequentially during development, starting bipolarly and highly motile (A2B5 antigen). Neurites gradually extend (NG2 antigen) and multiply into process-bearing pre-myelinating OLs (O4 antigen) and subsequently into myelinating oligodendrocytes (MBP antigen)(figure 3) (69)

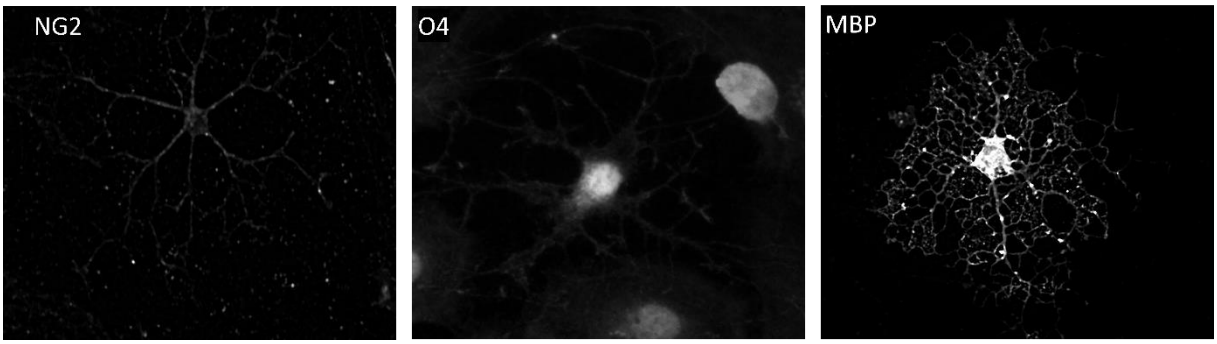

Figure 3: ***Developmental stages of oligodendrocyte development***

Immunodetection of NG2+ (left), O4+ (middle) and MBP+ (right) cells after day 3, 6 and 7 culturing in differentiating conditions, respectively. Bipotent glial progenitors (A2B5+ cells) were isolated by magnetic sorting from P2 mouse brain and seeded on poly-ornithine coated glasses in differentiating media.

We asked whether Grx2-deficient OPCs form aberrant contact sites with neurons, prior the formation of myelin sheath, and have an impact on OPC differentiation. For this we established a coculture with neurons and NG2+ cells isolated via magnetic cell sorting from whole mouse brain. First, sorted neurons were seeded and differentiated for 2-4 weeks to form a neuronal network. During this period NG2s were maintained in proliferating conditions and supplemented with bFGF and PDGF-AA mitogens. At the day of co-culturing, media was changed to support OPC differentiation and supplemented with T3/T4 hormones. After indicated period, cultures were fixed and visualized by immunostaining. Sorted NG2+ cells were characterized with different markers (see figure 4). Oligodendrocyte lineage transcription factor 2 (Olig2) antibody stains OL during all developmental stages (69). In Figure 4A OL are stained with Olig2 (magenta) and neurons with anti-b-III-tubulin (cyan). A few multipolar star shaped cells can be seen in a morphological shape known for pre-myelinating OL (69). MBP+ cells (magenta/white figure 4B) form multiple branches and have a spider web like formation. Unexpectedly, anti-β-III-tubulin (Tuj1 clone) also immunostained OLs but due to shape and structure, these cells can be distinguished from neurons. In another approach anti-NG2 antibody was added to visualize early stages of OPCs (yellow in figure 4C). Multiple process bearing cells can be seen either in green, yellow or cyan. Green forms through an overlapping of Tuj1 (cyan) and NG2 (yellow). Notably, even at a late stadium (42-days neurons, 37-day OPCs) NG2+ cells were still present in cultures (see figure 4C). For further characterization of the role of Grx2 in oligodendrocyte development this approach was developed to establish neuron-OPC co-culture with cells isolated from conditional tamoxifen inducible Grx2 knockout mice (CSP4-CreERT2/GRX2-LoxP lineage), in which expression of Cre recombinase is driven by *CSP4* (NG2) promoter.

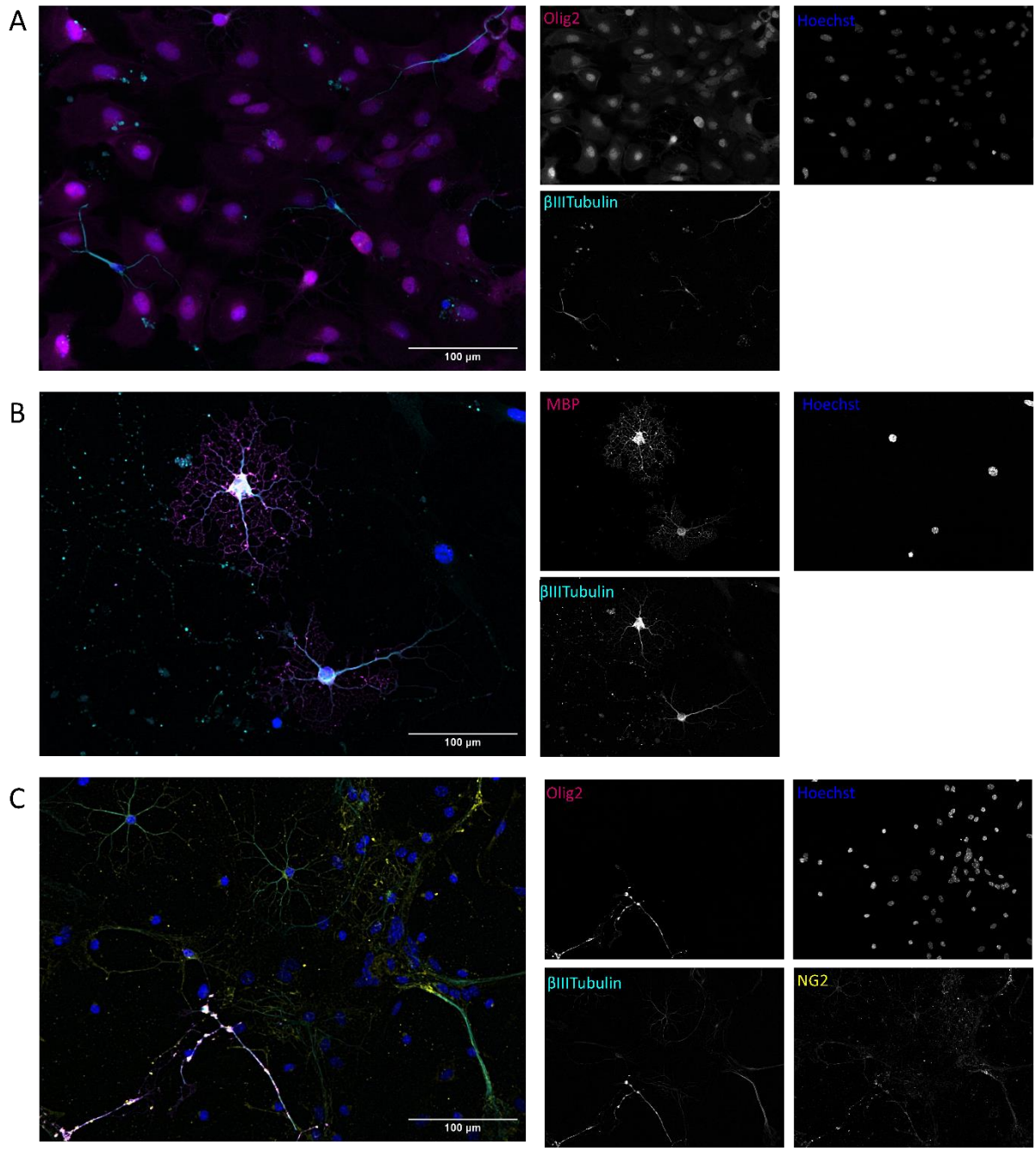

Figure 4: ***OL stages in co-cultures***

Immunodetection of neural cells in co–cultures ***A)*** *34 day neurons/6 days NG2+ cells: Stained for Olig2 (magenta), β-III-tubulin (cyan) and hoechst (blue)* ***B)*** *34 day neurons/6 days NG2+ cells: Stained for MBP (magenta), β-III-tubulin (cyan) and hoechst (blue)* ***C)*** *42 day neurons/36 days NG2+ cells: Stained for MBP (magenta), β-III-tubulin (cyan), NG2 (yellow) and hoechst (blue). Scale bar 100 µM.*

I applied the condition enabling the successful recombination of *Grx2* gene by using tamoxifen that has been previously established in the lab (C. Berndt unpublished data). NG2+ were treated with 1 µM tamoxifen for 48 hours and added to a 4-week-old neuronal

culture as described above (figure 5A). Tamoxifen induces CSP4-CreERT2 to delete the *Grx2* gene. Control cultures were treated with vehicle (ethanol) and rerun in parallel. Images were taken after 4 days (figure 5D) and after 6 days (figure 5B, C) after plating of NG2+ cells to neuronal cultures. Contact sites between OL and neurons were detected in both groups. Generation of MBP+ cells was diminished in tamoxifen-treated group (13%) as compared to vehicle group (22%) (p=0.049; n=4) (figure 5B). Tamoxifen-treated group significantly showed more Olig2+ cells (83 % versus 59 % in vehicle group p=0.0215) (figure 5C). Taken together, inducible deletion of Grx2 (a and c isoforms) may affect OPC differentiation (or MBP expression), however did not show an impact on contact formation between neural cells.

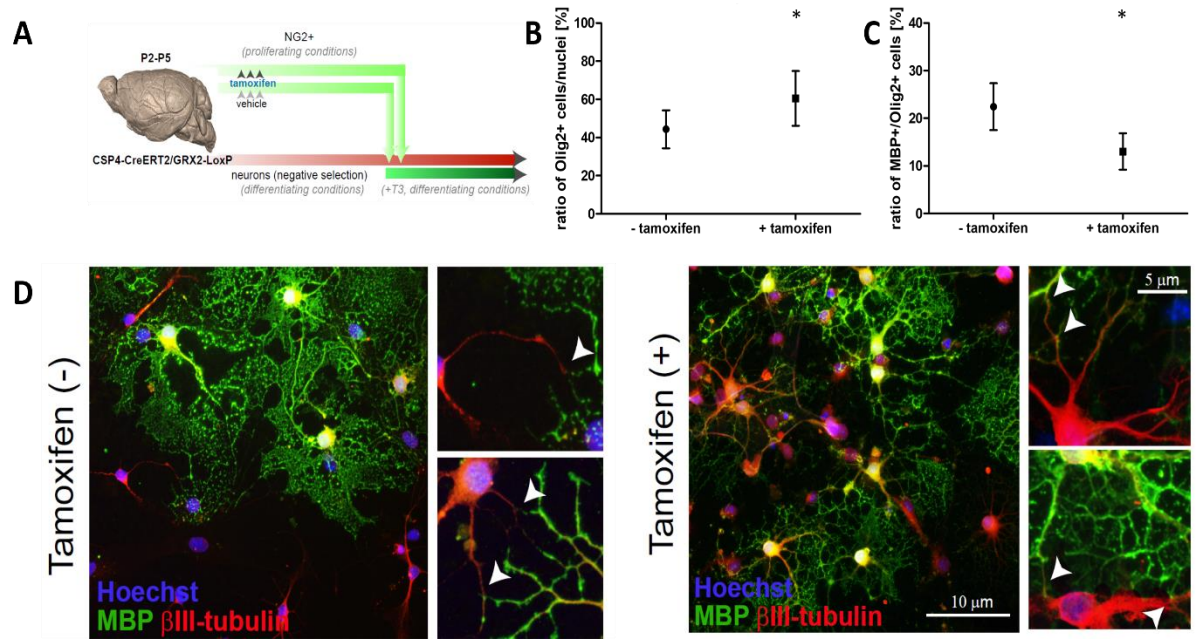

Figure 5: ***Effect of Grx2 deletion in OPCs on oligodendrocyte differentiation and contact formation***

A) *Schematic presentation of co-culture preparation with tamoxifen-induced gene deletion* ***B)*** *Ratio of Olig+ cells and nuclei stained with Hoechst and* ***C)*** *Ratio of MBP+/Olig+ cells in tamoxifen induced and control co culture (34 days neurons/6 days NG2+ cells). A one tailed paired t-test was conducted (* p<0.05 n=4)* ***D)*** *Immunodetection of tamoxifen induced and control co-culture (32 days neurons/4 days NG2+ cells). Cells were stained against MBP (green), βIII-tubulin (red) and hoechst (blue). Contact sites between oligodendrocytes and neurons (depicted by arrowheads) can be seen in both groups. Scale bar 10 µm (right panel) and 5 µm (left inserts)*

In summary, this co-culture model will be useful for examination of OPC-neuron interactions at early stages and molecular characterization of contact site formation. The exact time points and cell numbers remain to be examined to improve visualization of contact sites.

4.2. Effect of Grx2c on mitochondrial membrane Potential

The mitochondrial membrane potential (MMP, $\Delta\Psi m$) is a direct indicator for mitochondrial activity (70) and generated through proton pumps of the ETC (complex I, III and IV) (71). Stem cell differentiation is guided by mitochondrial metabolism, which is influenced by the MMP (72). OPCs have a high metabolic demand that requires mitochondrial ATP and carbone-backbone production during the formation of lipid-rich membrane proteins (needed for myelination), while they rely less on mitochondrial respiration after myelination is complete (discussed in (73)). Grx2a was shown to (de)glutathionylate the mitochondrial complex I in different cell types (e.g. lens epithelial cells (26), cardiac and liver tissue (32)). Thus, in addition to various signaling cascades (e.g. Crmp2 (10), SIRT1 (14)) regulated by Grx2 in redox-dependent manner, Grx2 may contribute to mitochondria-dependent events during NSC- and particularly OPC-differentiation program. To this regard, we first aimed to analyze whether the MMP; generated by proton pumps (Complexes I, III and IV) is affected in Grx2 lacking cells (Grx2 KO) and if recombinant hGrx2c can influence the MMP.

MMP in wild type (WT) and Grx2 KO (Grx -/-) mouse embryonic fibroblasts (MEFs) were measured to validate a change in mitochondrial membrane potential. The used measurement is based on a cell-permeable dye which emit fluorescence at 535 nm (green) in inactive mitochondria. Polarization of the mitochondrial membrane leads to accumulation of the polar dye which then changes it fluorescence at 590 nm (orange). For this purpose, WT and Grx2 KO MEFs were analyzed in a black 96-well plate. Cells were incubated over night after seeding $2x10^5$ in triplicates. Dye emission ratios (590/535 nm) were measured to demonstrate that he MMP is independent from the number of mitochondria. In Grx2 MEFs the MMP was decreased by 40 % (figure 6, $p=0.0014$) supporting the results of other groups, wherein Grx2 increases mitochondrial activity through the deglutathionylation of complex I. As expected the positive control (CCCP treated) can't build a proton gradient and has therefore a low MMP.

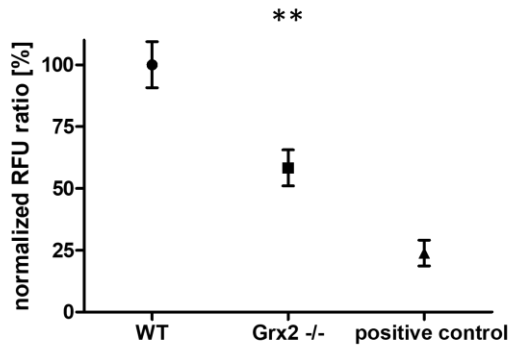

Figure 6: ***Effect of Grx2 KO in MEFs***

*Normalized relative fluorescence units (RFU) at 590/535 nm of wildtype (WT), Grx2 knock-out (Grx2 -/-) and CCCP treated (positive control) MEFs. A one-winged unpaired t test showed significant reduction of MMP for Grx2 -/- (** indicates P<0.01 n=3).*

Next, we measured the MMP at different stages of OPC differentiation. NG2-positive and O4-positive cells were sorted from P2 whole brain lysates (C57B6 mouse strain), and were seeded in a black 96 well plate for seven days in proliferating conditions to maintain undifferentiated state. The remaining cells, which where eluted following positive-sorting for NG2 and O4 markers, were recovered in the presence of bFGF/EGF in a petri dish. Free-floating neurospheres (represent NSC population lacking bipolar O2A and OPC progenitors) formed after six days, were collected, dissociated, and then added to the 96 well plate in WT and Grx2 KO. At day seven, MMP was measured and plotted (figure 7). To avoid the influence of different number of cells on measured parameters we applied a normalization approach (see method part). Data showed the highest MMP for stem cells (100 %), followed by NG2 glia cells with 88 %. O4 positive cells were characterized by decrease in MMP up to 51 % as compared to NSCs. $Grx2^{-/-}$ NSCs exhibit drastic reduction in MMP comparable with NSCs treated with 4 µL inhibitor, CCCP. Data was taken in triplicate but vastly varied inside one group, probably due to high fluctuations in the cell count.

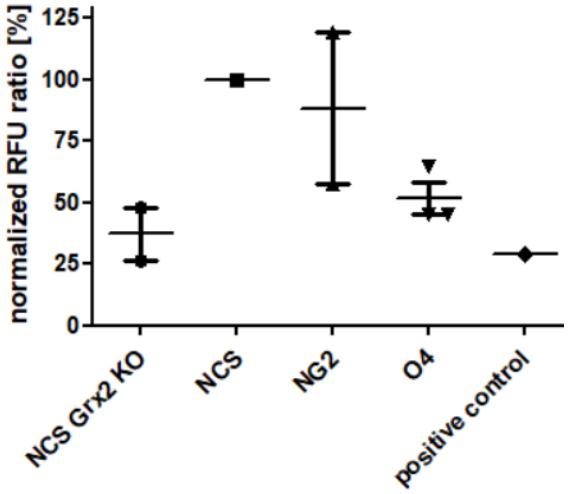

Figure 7: ***MMP in OL stages and NSCs***

Different cell populations were isolated from P2 mice brain via magnetic cell sorting, seeded on a 96-well plate and measured with the MitoID. Normalized relative fluorescence units (RFU) at 590/535 nm of O4+ and NG2+ wildtype (WT) cells, CCCP treated WT NSCs (positive control), WT NCSs and Grx2 -/- NSCs. Data was taken in triplicate but vastly varied inside one group, invalidating some values. T-test couldn't be conducted due to loss of replicates.

This pilot experiment demonstrates that similar to other cell types examined (see above), Grx2-deficiency strongly impacts mitochondrial activity and is not full compensated by other redoxins in neural cells. Taking into account the key role of mitochondria in OL maturation, the drop in mitochondrial activity in Grx2-defficient progenitors may impact the generation of myelinating cells observed in previous experiments with inducible Grx2 knockout (Figure 5). Nevertheless, the experiment needs to be further optimized, particularly in regard of sorting conditions and recovery period that may affect cell homeostasis in general. Taken together, the role of Grx2 in mitochondria activity may argue for a novel mechanism by which Grx2 (or redoxins) influence cell intrinsic program of cell differentiation.

4.3. Effect of recombinant hGrx2c on synaptogenesis

Synapses are contact sites between neurons formed in a later stage of development, enabling the transmission of information between neurons (74). As mentioned previously, recombinant cytosolic human Grx2 (rhGrx2c) was shown to enhance axonal outgrowth and axon guidance by reducing CRMP2 and, thus, interacting with the semaphorin-3A-plexin pathway (10). On the other hand, CRMP2 mediates Sema3F-

dependent axon pruning and dendritic spine remodeling (75) as well as synaptic plasticity. CRMP2 is a synaptic protein, expressed at pre- and post-synaptic sites. Interactions with proteins such as N-methyl-D-aspartate receptors, syntaxin1A as well as voltage-gated calcium and sodium channels, suggest that CRMP2 may control both the electrical and chemical components of synaptic transmission (76). Recently, it was demonstrated that CRMP2 interacts with Drp1 and Miro2, proteins involved in regulating mitochondrial dynamics (mitochondrial morphology and motility) and play a major role in the proper functioning of distant synapses (77). Therefore, we asked whether synaptogenesis can be modulated in the presence of rhGrx2c.

Hippocampal mouse neuronal stem and progenitor cells (NSPCs) were generated as described in methods (chapter 3.2.3. Isolation, maintenance and differentiation of cells) from P2-P5 mice and were grown in different conditions to enable generation of mature neurons. Supplementation with conditional media (media gained from astrocyte cultures) with FCS showed the best neuronal growth as seen in figure 8. Images were acquired with LAS X software and the LEICA TCS SP8 confocal microscope (60 x magnification).

Figure 8: ***Visualization of 14 days old neurons***

Immunodetection of 14 days old neurons differentiated from hippocampal NSPCs in the presence of conditional media from astrocyte cultures. Neurons were stained with SMI-31 against neurofilament H. Scale bar 30 µM

Synapses can be visualized by using antibodies against pre- and post-synaptic proteins. Overlapping of both signals is assumed to indicate a functional synapse formation. (62). Figure 9A shows 13 days old neurons stained for homer1 (post-synaptic) and synapsin1/2 (pre-synaptic) proteins. Both markers are mostly co-localized, go along neurites and also accumulated in the cell soma (neuronal body). Additionally, SMI-31 was used to visualize axons by staining for neurofilament H, despite the soma and some neurites were also detected. A clear contact site can be seen between two neurons, however the background signal hindered quantification of synapses. Detection of synapse formation was further improved with an optimized protocol for ICC as described in methods (chapter 3.2.4. immunocytochemistry). As shown in figure 9B, homer1 is distributed mostly around the soma of neurofilament-negative cells with bigger nuclei (characteristic of astrocytes) and neurites. Synapsin 1/2 were expressed along the neurites. Although, a better resolution of synapse is required, co-localization of both, pre- and post-synaptic proteins on two different neurites, are observed (bright pink and white spots). Staining could be optimized but synapses still couldn't be quantified du to overlapping signals.

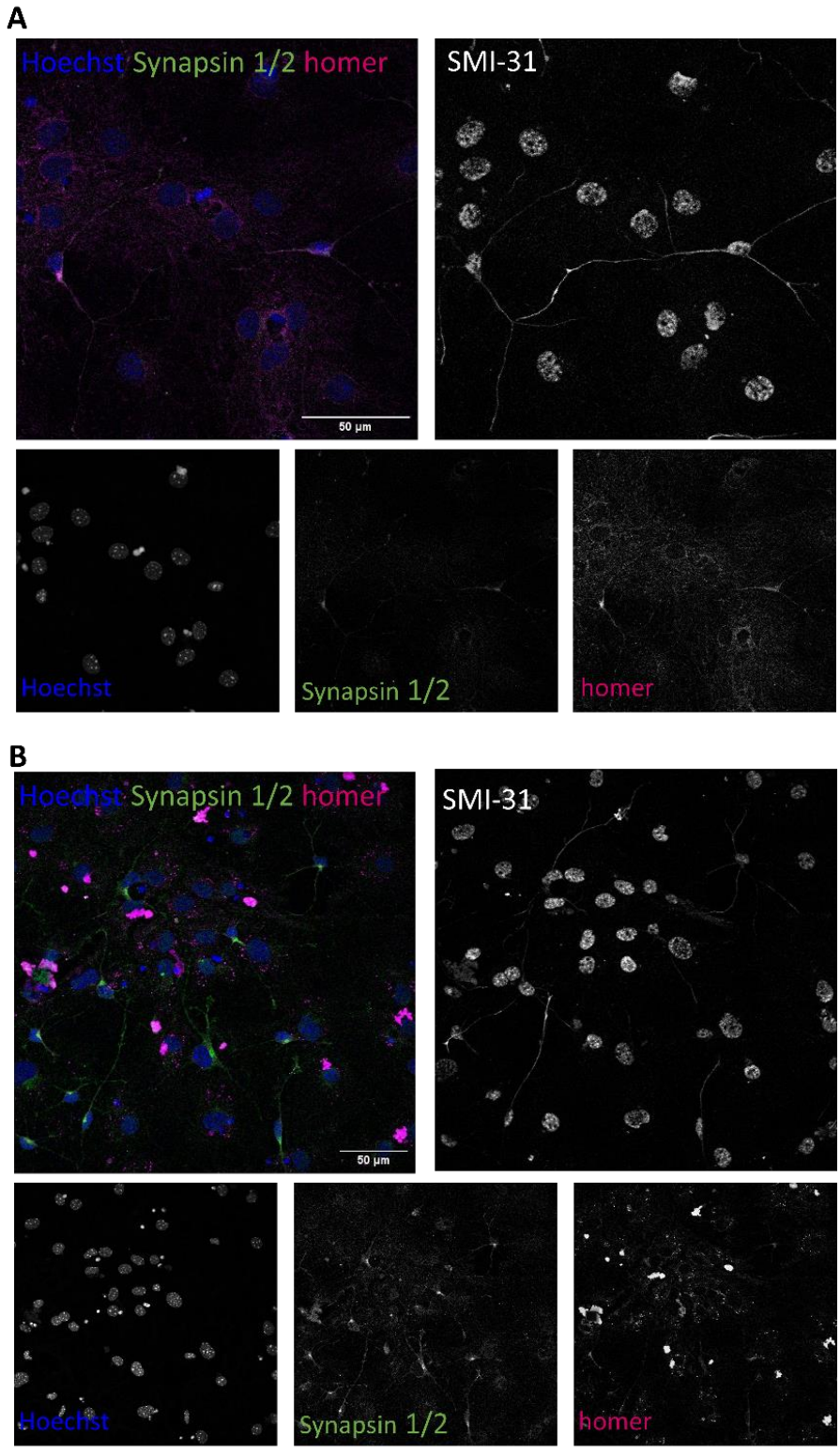

Figure 9: ***Neuronal synapse visualization***

Immunodetection of 13 days old neurons differentiated from hippocampal NSPCs (two different cultures) in the presence of conditional media from astrocyte cultures. Neurons were stained against homer1 (post-synaptic, magenta) and synapsin1/2 (pre-synaptic, green) proteins overlapping to bright pink and white. Additionally, SMI-31 was used to stain neurofilament H. ***A)*** *old ICC protocol* ***B)*** *optimized ICC protocol. Scale bar 50 µM.*

In order to optimize the protocol for enrichment of pure population of neurons, the following protocol was examined. NSPCs were first sorted out from A2B5-positive cells (to exclude glial precursors) and then additionally immunosorted for PSA-NCAM (polysialylated neuronal cell adhesion molecule), a marker of developing and migrating neuronal progenitors (78). Sorting was started with 6 million cells while $2x10^5$ PSA-NCAM positive cells (30% of total NSPCs) were obtained. Cells were seeded in two conditions. One group was treated with arabinoside C to reduce the amount of proliferating cells (predominantly contaminating glial cells). However, a toxic effect of treatment on neuronal population was observed in several experiments. Another group was grown in the presence of astrocytes, while astrocytes formed a matrix on the titer plate and neurons were seeded on poly-ornithine coated glasses and inserted in culture inlays (without physical contacts with astrocytic feed layer). Unfortunately, this approach was unsuccessful to generate neurons that would firmly attach to glass surface.

The performed experiments couldn't elucidate any impact of Grx2c impact on synaptogenesis. The protocol still needs optimization, in particular the generation of homogenous neuronal networks. Furthermore, a semi-automated protocol needs to be established in order to quantify the co-localization of synaptic markers.

4.4. Effect of Grx2 on neurite outgrowth in SN4741 cell line

We asked whether rhGrx2c, known to promote axonal outgrowth through the CRMP2 pathway, may also affect growth of neurites. For this, SN4741 cells (mouse dopaminergic cell line) were seeded on poly-L-ornithine-coated cover glasses and exposed to differentiating conditions (1 % FCS, 39 °C) according to Son and colleagues (61). One group was treated with 2 µM hGrx2c and another left untreated. Media was exchanged every 2nd day completely and 3 cover glasses of each group were analyzed on day 1, 3 and 9. Neuronal cells were stained for β-III-tubulin and counterstained with Hoechst, and images were taken with Olympus fluorescence microscope (20 x magnification) (figure 10).

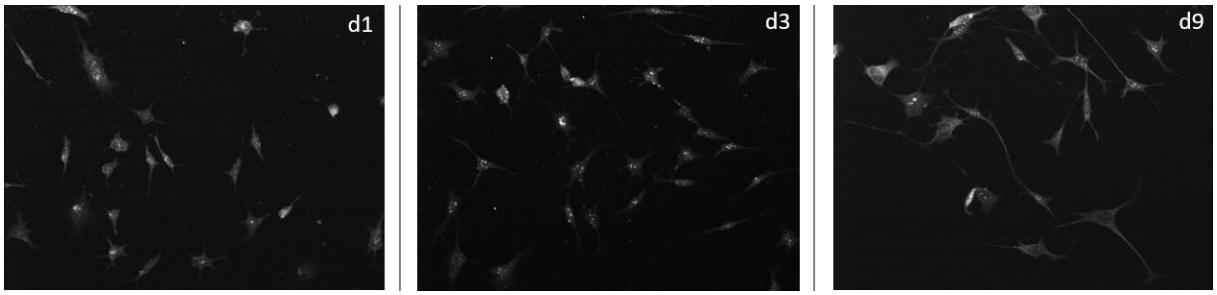

Figure 10: ***Growth of SN4741 cells***

Immunodetection of untreated SN4741 cells during differentiation at day 1, 3 and 9. Neurites were stained for β-III-tubulin

Neurite outgrowth was quantified by measuring the pixel length of β-III-tubulin immunostaining by using NeurophologyJ software and its feature Simple Neurite Tracker (SNT), a plug-in for Fiji (79). Fluorescence images were acquired on five locations on each cover glass. In a total of 15 images per group, 10 dendrites were measured with SNT. Quantification was done semi-automatically by marking the start and end point of dendrites. The plug in then automatically fills the path and calculates the pixel distance. The mean of the longest five neurites per image were calculated and the 7 highest mean values in every group were used for analysis. Normalized data was plotted in GraphPad prims5 and a one-tailed unpaired t-test was performed (figure 11). SN4741 cells grew neurites over the period of nine days, while growth was faster in the first days. From day 1 to day 3, overall neurite length was increased by 38 % and from day 3 to 9 only 26 %. Grx2c-treated and untreated groups didn't show any difference in neurite lengths, concluding that hGrx2c didn't influence neuronal outgrowth in dopaminergic SN4741 neuronal cells.

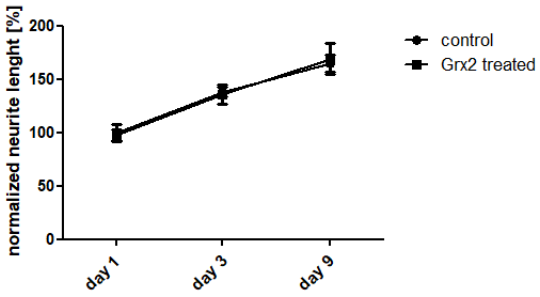

Figure 11: ***Effect of rhGrx2c on SN4741 neurite outgrowth***

Treated (2 µM rhGrx2c) and untreated SN4741 cells were grown for 9 days and ICC was conducted on day 1, 3 and 9. Neurite length in pixel was quantified in every group using Fiji (NeuroanatomyJ and SNT plugin). No significant changes could be calculated

4.5. Effect of Grx2 on DKK1 and p53

The redox shift assay can be used to detect the *in sit*u redox state of a specific protein of interest via tagging of reduced thiol moieties with a methoxypolyethylene glycol chain substituted maleimide probe (mmPEG). The probe has a defined mass (e.g. 1 kDa) and therefore increases the overall mass of a protein depending on the number of reduced cysteines present. In an SDS-PAGE analysis with immunodetection of the protein of interest, the protein appears shifted towards higher molecular weight depending on the amount of tagged thiol moieties. Two approaches are possible with the redox shift assay. Immediate tagging of reduced thiols after isolation of protein (direct redox shift assay) or blocking of reduced thiols *in situ* and later tagging of oxidized thiols (indirect redox shift). The later approach is overall superior since blocking is done *in situ*. Still blocking can be insufficient due to hydrophobic or sterically hindered sides in the protein structure and results must be discussed with care.

The Wnt signaling pathways regulate a spectrum of developmental programs like cell migration, neuronal patterning and cell polarity (80). Particularly, development and differentiation of dopaminergic neurons (81) as well as their in vitro model SN4741 cells (82) are tightly coordinated by the Wnt signaling. Dickkopf related protein 1 (Dkk1) is a secreted inhibitor of WNT signaling with two cysteine rich regions influenced by ROS signaling (83) that plays a role in neuronal differentiation towards dopaminergic lineage (84). We asked whether hGrx2c can alter the redox state of Dkk1 and conducted an indirect redox shift assay to determine the oxidation status by using western blotting approach. SN4741 cells were seeded in a 6 well plate ($5x10^5$ cell per well) in DMEM with 0.1 % FCS. The next day, medium was refreshed and 1 mM LiCl (activator of Wnt signaling and inducer of Dkk1 (85).was added to every well. One group was treated with 2 µM hGrx2c. 6 hours later supernatant was removed and cells were treated as described in methods (chapter 3.2.8. indirect redox shift). (66)

Here the indirect redox shift was used to detect the redox state of Dkk1 after treatment with Grx2. In it, reduced thiols in the protein first are blocked using N-ethylmaleimide (NEM) *in situ*. Afterwards, cells are lysed and proteins denatured using SDS containing buffer. Then Tris(2-chlorethyl)phosphate (TCEP) is added, which converts all TCEP reduceable thiol modifications (e.g. not-NEM tagged) to the reduced cysteine. Finally, all TCEP reduced thiols are being tagged by incubation with methoxypolyethylene glycole

maleimide (mmPEG). The minimal shift group has all thiols reduced and blocked with NEM, while all thiols are modified with mmPEG in the maximal shift group. (66)

After treatment, tagged protein cell lysates of each sample were separated via SDS-PAGE and subsequently redox state of Dkk1 (figure 12A) was analyzed using immunodetection methods. Mouse Dkk1 has a molecular weight of 29 kDa (UniprotID 054908). The maximal shift (all cysteines modified with mmPEG) shows a band at 35 kDa indicating successful maleimide modification of most cysteines. The minimal shift cannot be identified due to insufficient protein separation (but should appear theoretically next to the unmodified group). Steady state samples show the physiological redox state of Dkk1 with a band at around 28 kDa and a second band at around 35 kDa, suggesting two populations of distinct redox states of Dkk1 in the cell. In densitometry analysis, the ratio between more reduced and more oxidized Dkk1 is stable in all treatments at 5:4 reduced to oxidized state. This assay indicated for redox modifications of Dkk1, however Grx2 didn't affect the redox state of Dkk1. (66)

The same blot was co-immunostained for p53, a 53 kDa protein, apart for its role in cell cycle arrest and apoptosis ("guardian of the genome"), known for regulating neuronal differentiation (86) (figure 12B). p53 activity is modulated via redox regulation (87). Here we tested whether hGrx2c might has an impact on p53 redox state. The maximal shift shows a clear shift to 70 kDa, while the minimum appears at 53 kDa. Steady state groups are slightly higher and are thus modified with mmPEG, indicating for redox modulation of p53, however not facilitated by Grx2.

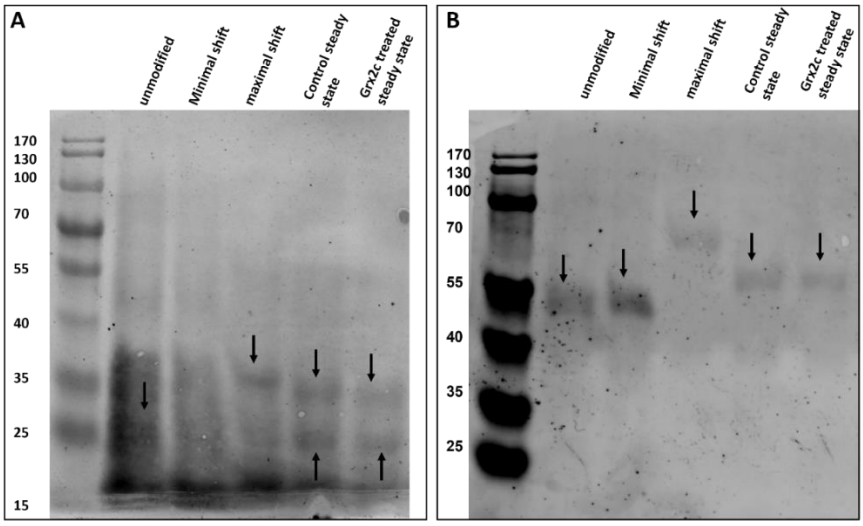

Figure 12: ***Effect of rhGrx2c on redox state of Dkk1 and p53 in SN4741 cells***

SN4741 one cells were treated with 1mM LiCl and group with 2 µM rhGrx2c for 6 hours. Steady state samples were blocked in situ with NEM. All groups were then treated with TCA, solubilized with Laemmli buffer and treated with TCEP to reduce disulfides. Then unmodified group was left untreated, the minimal shift was treated with NEM to trap all reduced cysteines and the remaining groups with mmPEG to modify reduced and untrapped cysteines. Protein lysates were then separated via SDS-PAGE and analyzed with western blotting. ***A)*** *DKK1 antibody (35 kDa) at 680 nm and* ***B)*** *p53 antibody (53 kDa) at 800 nm. The band of steady state samples is below the maximal shift for both proteins.*

4.6. Human iPSC derived NSC culture. Does treatment with recombinant Grx2 triggers mitochondria activity?

Supplementation with Grx2c promotes axonal outgrowth in CRMP2-dependent manner (53). As mentioned above, CRMP2 interacts with Drp1 and Miro2, proteins involved in regulating mitochondrial dynamics and functions (mitochondrial morphology and motility) (see 69). Results of previous experiments (see above) and published data from other groups point to the key role of Grx2 in mitochondrial homeostasis. Therefore, we aimed to examine the effect of rhGrx2c on mitochondrial activity of developing neurons. To this aim, we first established a human NSC culture derived from iPSC.

NPCs differentiated with small molecules from human induced pluripotent stem cells (namely smNPC) are of great interest for stem cell research and regenerative medicine. We implied and established protocols to culture, differentiate and study smNPC in our lab. smNPCs were first generated by Carmen Menacho-Pando (AG Prof. Dr. Alessandro Prigione). Survival after thawing of cryo preserved cell stocks and cell proliferation

demonstrated a vast difference between six batches of cells. Therefore, the results presented below indicate a data produced from single cell batch. Clusters of colonies and long neurites formed over the time of 21 days (figure 13). During fixation with PFA and following washing steps on the orbital shaker, vast majority of cells detached from the cover glasses along with Matrigel (used to support cell growth) (indicated with arrows in 15). This general problem did not allow visualization and characterization cell subsets by using immunocytochemistry.

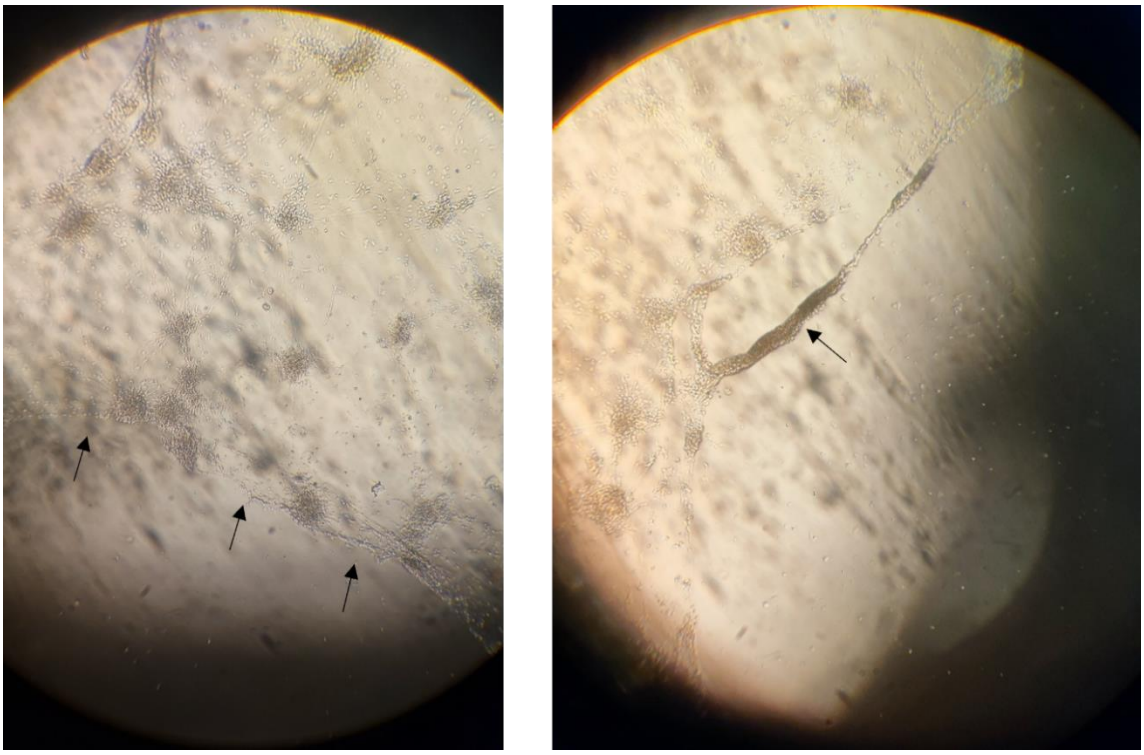

Figure 13: ***smNPC culture at day 19***

Differentiating smNPC after fixation at day 19 and first antibody stain. Images were taken with a Xiaomi Mi10T Pro smartphone through the lens of a brightfield microscope (4x magnification)

Cells were seeded in a black 96 well plate in triplicates and differentiated for 19 days in the presence or absence of recombinant hGrx2c. MMP was measured at day 7, 14 and 19. It is important to mention, that although being exposed to differentiating conditions (see Methods), cells still maintained their mitotic activity and crowded the wells leading to enriched confluence. 100 % confluency was reached at day 14. Emission ratios (polarized mitochondria versus inactive mitochondria) were measured and plotted (figure 14). hGrx2c-treated cells exhibited an approximately 20 % (Day 7; p=0.084) and 18% (day 14,

p=0.0056) increases in MMP as compared to control (untreated) group. This difference disappeared at day 19, when cell cultures (in all groups) were overgrown and starved. Drastic changes in cell number due to active mitotic state of progenitor cells did not allow to accurately evaluate the kinetic of mitochondrial activity upon differentiation. Nevertheless, the effect of recombinant hGrx2c on mitochondrial activity in NSCs is in line with previous experiments and indicate a novel mechanism by which glutaredoxin may regulate the differentiation program of NSC.

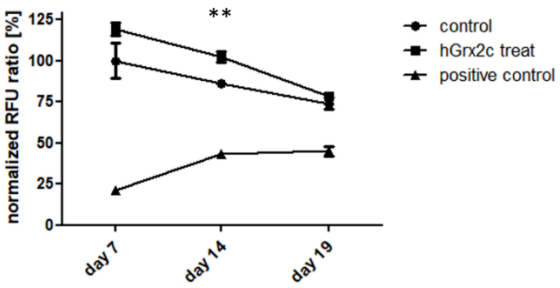

Figure 14: ***Effect of rhGrx2c on smNPC MMP***

*Normalized relative fluorescence units (RFU) at 590/535 nm of smNPC (control), 2 µM hGrx2c treated and 4 µM CCCP treated (positive control). Data were collected at days 7, 14 and 19 of differentiation. A one-winged unpaired t test was conducted (** indicates p<0.01).*

4.7. Effect of Grx2 on NMDA induced currents

The effect of rhGrx2c (supplemented in growth media) on mitochondrial activity in neural cells prompted us to examine the novel cell surface molecular targets of its activity. CRMP2, a known target of Grx2, implicated in NMDA-mediated synaptic transmission (68) and NMDAR signaling may serve as an attractive candidate directing Grx2-mediated effects. N-methyl-D-aspartate receptors (NMDAR) are ionotropic glutamate receptor controlling synaptic plasticity and memory function (86). NMDAR signaling in OPCs was proposed as a power switch in upregulation of mitochondrial metabolism by the mechanism dependent from an influx of calcium ions (87, 88). We hypothesized that treatment with recombinant hGrx2c may influence redox state of NMDARs and by this regulate NMDAR signaling, and ultimately, the mitochondrial activation. Cell-permeable dyes, including Fura-2AM and mitoSOX, were used to quantify intracellular Ca^{2+} and mitochondrial superoxide levels respectively in response to NMDA, kainate or glutamate treatment. Upon reaction with their target, the non-fluorescent dye gets activated and fluorescence emission can be measured with a plate reader. For this NG2+ positive cells,

that express NMDARs and exhibit NMDA-evoked currents (89) were prepared as described in methods (chapter 3.2.3.). One group was treated with 0.8 mM GSH (control), another with 0.8 mM GSH and 2 μM rhGrx2c (treat), in order to maintain active state of glutaredoxin. There was no significant difference in calcium concentrations between control and treated groups in the beginning of measurements (2-5 min) (figure 15 A). The same cells were measured 20 min later with no difference in both groups but a general increase from around 15 to 70 nM Ca^{2+}. The latter is in line with a role of glutathione in NMDA-mediated neuronal transmission (90)and modulation of redox sites of NMDARs that may occur at basal (non-induced) conditions. Afterwards both groups were treated with 100 μM glycine, which acts as a co-binder for NMDARs (91), followed by application of 10 μM NMDA, or 100 μM glutamate or 10 μM kainite in three separate subgroups of each rhGrx2c and control group (figure 15B). Here again, no difference could be seen between the groups. To determine the maximal Ca^{2+} influx capacity and Ca^{2+} concentrations (Ca^{2+} load) cells were treated with 26 μM ionomycin and emission was measured. The same cultures were assessed for mitochondria-derived superoxide production (delayed long-term effect). Each well was replenished with proliferation media and cells were incubated overnight at 37 °C. The next day we conducted a mitosox assay as described in methods to elucidate the effect of NMDAR stimulation on mitochondria activity (figure 15C). Glutamate and kainite treated groups showed similar fluorescence units while NMDA treated cells had significantly (P=0.0001) higher fluorescence intensity than the other subgroups. Of note, previously it has been shown that neuronal NMDAR stimulation triggers superoxide production via activation of NADPH oxidase complex (NOX) (92) and the localization of oxidized dyes to the mitochondria does not itself establish that mitochondria are the source of oxidant production, as demonstrated by oxidation of mitoSOX in neuronal mitochondria by xanthine/xanthine oxidase added to the culture medium (93). Therefore, a caution has to be taken for interpretation of NMDA-induced superoxide source in OPCs.

Cultures treated with GSH developed an overall reduction in mitosox-based fluorescence in agreement with its ROS scavenging effect. No additional effect was observed in cultures with applied GSH+hGrx2c. After treatment with neurotransmitters, superoxide levels increased (immediate effect), supporting the role of superoxide in neurotransmitter-induced signal transduction as an intercellular messenger (94). Treatment with rhGrx2c

did not affect intracellular calcium and mitochondrial superoxide anion levels but treatment with 40 µM NMDA (for 1 h) lead to a long-term effect with increased superoxide anion concentration even after 16 h.

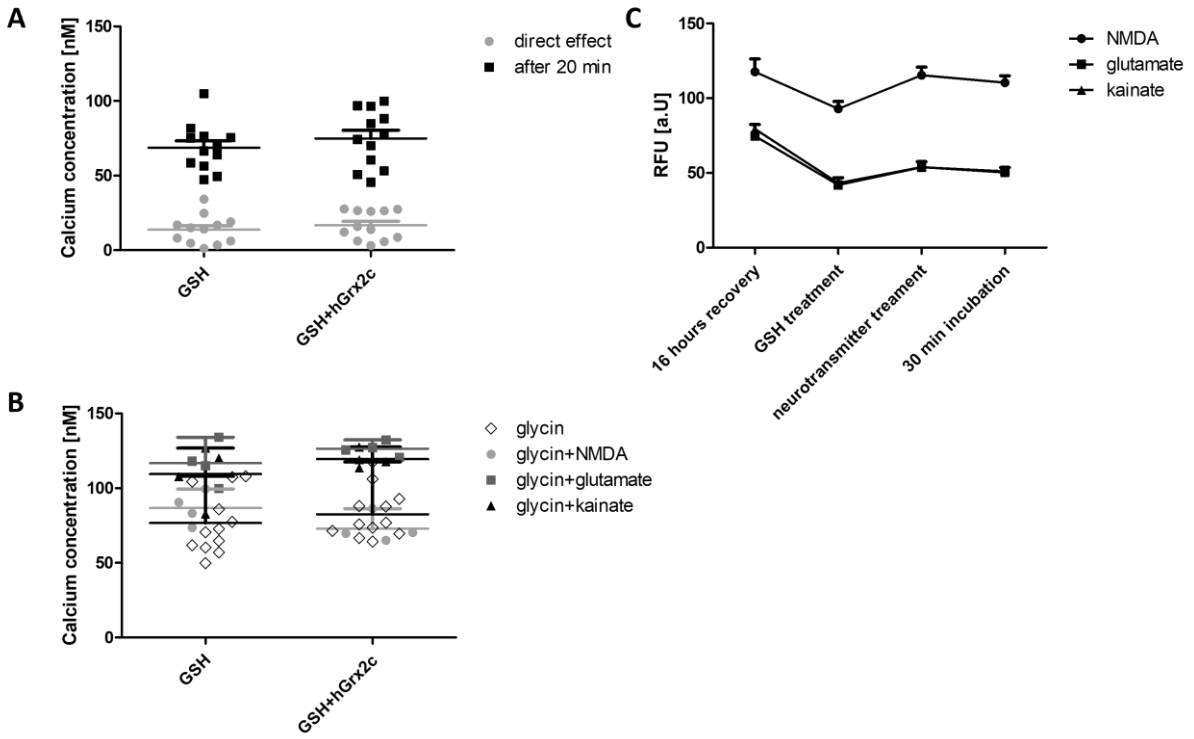

Figure 15: ***Effect of rhGrx2 on Ca^{2+} and superoxide levels in NG2+ cells***

Ca^{2+} concentration measured with Fura2-AM in sorted NG2+ cells ***A)*** *after 2 µM rhGrx2c treatment and after* ***B)*** *treatment with 100 µM glycine and further 10 µM NMDA, 100 µM glutamate and 10 µM kainite.* ***C)*** *relative fluorescence units of MitoSOX in NG2+ after 16 hours of recovery and further treatment with 0,8 mM GSH, with neurotransmitters named in B and after further incubation of 30 min*

5. Discussion

Several studies suggest Grx2 as a major mediator of redox signaling, directly interacting with redox switches of the exposome to respond to environmental changes and cell-intrinsic cues. Molecular targets of Grx2, including mitochondrial complex I, Sirt 1 and CRMP2 among many others, are the key components in the process of neural stem cell differentiation. Thus, Grx2 can be considered as a vital player orchestrating parallel processes required for proper cell fate and development. In the present study I investigated the morphological changes and metabolic activities in neural stem/progenitor cells deficient for Grx2 or treated with recombinant hGrx2 to further identify the potential mechanisms underlying the effect of the enzyme. I show that the overall number of NG2+-derived Olig2+ cells were increased in tamoxifen induced Grx2 KO primary cultures, while the number of myelinating MBP forming cells was decreased. Investigation of mitochondrial activity of Grx2 KO in MEFs and NSCs revealed a drastic decrease in MMP, while rhGrx2c treatment was associated with enhancement. I conclude that GRX2-dependent regulation of mitochondrial dynamic as well as homeostasis is a novel mechanism by which glutaredoxins are involved in NSC biology.

In general, thioredoxins (oxidoreductases) and thioredoxin reductases regulate many aspects of NSC functioning including neurite outgrowth (95), proliferation (96) and survival (97). Although many signaling pathways were identified as a primary targets of oxidoreductase action, their role in mitochondrial dynamics upon differentiation was underestimated. The results of present work are consistent with recent studies with Grx2 KO models in skeletal muscle cells, hepatocytes, cardiomyocytes and zebrafish showing aberrant development (56, 32, 41, 51).

One of particular interest in present study was addressed to the role of Grx2 in OPCs. NG2+ cells are present throughout of live in the brain in undifferentiated state playing various physiological role by mechanically communicating with neurons and providing an endogenous pool of OPCs for myelin regeneration, a major hurdle in demyelinating diseases such as multiple sclerosis (MS). In pure in vitro cultures, OPC spontaneously differentiate into later OPC stages, while in neuronal co-cultures they are able to myelinate (98). One of the key questions in OPC biology is “what is the mechanism involved to maintain NG2 cells in immature state”. We have previously demonstrated that Grx2c increases NG2 expression via Sp-1 dependent transcription of *CSPG4* gene and in

parallel suppresses OPC differentiation (as suggested by decrease in MBP+ cells) with unknown mechanism (54).In present study, I established a novel approach to examine the interaction and OPC differentiation in neuronal cultures. Co-cultures were produced by using tamoxifen inducible Grx2 knockouted mice (CSP4-CreERT2/GRX2-LoxP lineage). This in vitro model gives a possibility to study syngeneic cultures (derived from the same animal) by providing both knockout and WT neurons and OPCs. Supplementation with conditional media (secreted proteins from astrocytes) help to tackle one major hurdle of in vitro models (such as neuronal survival and growth) by mimicking the physiological microenvironment of neuronal precursors (99) and thus allows to generate neurons prior co-culturing with syngeneic OPCs. Number of non-neuronal and non-NG2+ cells were reduced by the usage of magnetic-activated cell sorting (MACS), however sorting procedure needs to be further optimized. Co-cultures proved to be useful in visualization and timely coordinated studies of contact sites between neural cells. As an outlook, co-cultures can be further optimized by virally introducing green fluorescent proteins (GFP) in neurons (100) or OPCs to distinguish between the two cultures. Here we demonstrated Grx2 knockout in OPCs leads to a moderate reduction of MBP expressing cells and an increase in Olig2+ population (Figure 5B, C). A potential explanation for the observed phenotype (e.g., diminished generation of MBP+ cells in Grx2 Ko) may point to the role of Grx2 in mitochondrial activity and dynamics. Schoenfeld et al demonstrate that oligodendroglial differentiation is accompanied by an increase of mitochondrial DNA content per cell and acetyl-CoA-related transcripts. Undifferentiated cells showed to be resistance against rotenone mediated inhibition of mitochondria while differentiated cell showed sensitivity to rotenone inhibition (101). This indicates that OPCs might maintain progenitor identity (low mitochondrial demand) to prevent dysfunction introduced during differentiation when mitochondrial function is needed to cover cellular demand. Grx2 deficiency leads to mitochondrial dysfunction and thus might favor oligodendrocytes to maintain earlier stages of development in addition to SP-1 dependent transcription.

Specific metabolic programs define cellular phenotypes (50). Stages during embryonic and NSPC lineage development are characterized inter alia by lipid metabolism, reactive oxygen species (ROS) signaling, and mitochondrial oxidative phosphorylation (OXPHOS)(44). A key factor for the metabolome are mitochondria. They dominate cellular

ROS production and subsequently prime the cellular redox homeostasis. Several studies suggest dysfunctional mitochondria at the basis of an imbalance in redox homeostasis playing a role in the progression of several neurodegenerative diseases (e.g., Alzheimer's disease) (102). In oligodendrocyte lineage, mitochondria prime the metabolome and provide metabolites for proper functioning of the cell, e.g. the synthesis of lipid-rich proteins to form myelin sheets. Grx2a was shown to modulate ROS production and mitochondrial activity through the (de)glutathionylation of complex I in different cell types (lens epithelial (26), skeletal muscle (30), liver, cardiac (41)). Here I can add two more cell types, in which mitochondrial activity is decreased in Grx2 knockouted cells, MEFs (Figure 6) and neural cells (Figure 7). In both cases MMP was measured and shown to be drastically reduced. Scalcon et al showed that in particular mitochondrial Grx2a is necessary for mitochondrial function and morphology (41). smNSC treated with rhGrx2c also showed elevated MMP which maintained for 12 days after withdrawal of rhGrx2c (Figure 14). Here we demonstrate that not only Grx2a but also recombinant Grx2c has an effect on mitochondrial activity (both differ in the intensity). Grx2c added to culture may regulate OPC differentiation not only through the SP-1 dependent CSPG4 transcription and reduction of CRMP2 but also by adapting the metabolome through modulating mitochondrial activity. Further emphasizing this hypothesis with the findings of Scalcon et al, who demonstrated that mice deficient in mitochondrial Grx2a have altered mitochondrial morphology and increased blood lipid levels, resembling the metabolic dysfunction-associated fatty liver disease (MAFLD) phenotype (41). Grx2a regulation of metabolic pathways was investigated but whether Grx2c can also be involved in that metabolic shaping needs to be further elucidated.

Grx2c has critical roles in cytoskeletal dynamic, cell adhesion and cancer cell invasiveness (53). In the present study, neurite outgrowth of dopaminergic SN4741 cells induced by heat shock-mediated cell cycle arrest was not affected by rhGrx2c (Figure 11), giving the question whether Grx2c regulation may be restricted to axonal growth or has a cell type specific effect. One target of Grx2c deglutathionylation is CRMP2 (10), a central component for specification of axon/dendrite fate and axon growth in neurons (103). CRMP2 is a mediator of Sema3A signaling and neuronal differentiation. Secreted Sema3A (collapsin-1) is known for repulsive guidance of axons and its ability to collapse the growth cone lamellipodium (104). In humans but not rodents, CRMP2 has two isoforms,

a long (CRMP2L) and short one (CRMP2S). CRMP2L is mainly expressed in neuronal soma and axons but not in dendrites, while the short one is mainly found in axons and dendrites (105) .Whether Grx2c-mediated effect on axonal growth is dependent on CRMP2 isoform and/or specious dependent is remained to be examined.

NMDAR activity is redox dependent and boosts activation of antioxidant mechanisms, including oxidoreductases (106). Multiple cysteine residues on the receptor composed of multiple subunits have been identified as a target for PTM. The addition of sulfhydryl reducing agents enhances NMDA-evoked currents, while oxidants showed the opposite effect (107), indicating for redox-dependent regulation of NMDAR function (108). In present study we did not find the effect of Grx2 on NMDAR-dependent Ca^{2+} influx or superoxide production, while our data support the role of glutathione in NMDAR signal transmission. Glutathione can attenuate neuronal damage induced by NMDAR activation (109) and was shown to increase NMDAR-induced influx of Ca^{2+} while GSSG had the contrary effect (110). In our experiment, NMDAR thiols were probably reduced through GSH and couldn't be targeted by deglutathionylation. Oxidation of NMDAR is required prior the addition of Grx2 to observe modulatory effects. If Grx2 can deglutathionylate NMDAR, then it might affect NMDAR activated upregulation of mitochondrial metabolites (87) to support cellular need, e.g. formation of myelin sheath, and would be directly involved in synaptic proteins. This would further emphasize our finding that number of MBP positive cells decrease in Grx2 KO culture, due to glutathionylated NMDAR inhibiting signal transduction to upregulate mitochondrial leading to an increase in the progenitor population. Additionally, Grx2a mediated mitochondrial impairment might block/delay differentiation into later stages which are dependent on mitochondrial activity. However, this needs to be further investigated.

5.1. Outlook

Accumulating evidence suggests thiol disulfides as key factors in the spatiotemporal regulation of differentiation and development. Grx2's ability to deglutathionylate and to reduce disulfides in a vast spectrum of substrates puts Grx2 in a position beyond maintaining cellular redox homeostasis. Grx2 might influence thiol redox homeostasis to maintain a specific cellular exposome in accordance with the momentary cellular need to

initiate and/or stabilize transition states during development and differentiation. Major developmental signaling pathways are modulated by glutaredoxin, its mitochondrial isoform can modulate mitochondrial activity and cellular metabolic programs, while the cytosolic isoform induces developmental signaling pathways through CRMP2, Sirt1 and SP-1 proteins among others. Its role in redox homeostasis and signaling make Grx2 a promising candidate for redox and regenerative medicine.

6. Acknowledgment

I would like to express my appreciation to PD Dr. Carsten Berndt for giving me the opportunity to write my thesis in his workgroup and Prof. Dr. Reichert for being my examiner.

I am particularly grateful for the assistance PD Dr. Tim Prozorovski provided me with and his willingness to give his time so generously. This also applies to Christian Kroll, who helped me with theoretical stuff and the practical work. Furthermore, I would like to thank everyone else in the group for sharing my frustration and motivating me to go on.

Special thanks to Prof Dr. Alessandro Prigione and Carmen Menacho Pando for providing me with smNPC and introducing me to this interesting field of research. Another thanks to PD Dr. Dr. Christopher Horst Lillig supporting my research with recombinant Grx2.

I also want to thank my family and friends for always being at my side and helping me out in times of crisis.

7. List of figures

8. List of tables

9. Literature cited

1. Buja LM. The cell theory and cellular pathology: Discovery, refinements and applications fundamental to advances in biology and medicine. Exp Mol Pathol 2021; 121:104660.

2. Ribatti D. Rudolf Virchow, the founder of cellular pathology. Rom J Morphol Embryol 2019; 60(4):1381–2.

3. Hansen JM, Jones DP, Harris C. The Redox Theory of Development. Antioxid Redox Signal 2020; 32(10):715–40.

4. Allen RG, Balin AK. Oxidative influence on development and differentiation: An overview of a free radical theory of development. Free Radic Biol Med 1989; 6(6):631–61.

5. Jones DP. Redox theory of aging. Redox Biol 2015; 5:71–9.

6. Berndt C. Redox Regulation of Differentiation and De-Differentiation. Milton: Taylor & Francis Group; 2021. (Oxidative Stress and Disease Serv.48). Available from: URL: https://ebookcentral.proquest.com/lib/kxp/detail.action?docID=6713901.

7. Sies H, Cadenas E. Oxidative stress: damage to intact cells and organs. Philos Trans R Soc Lond B Biol Sci 1985; 311(1152):617–31.

8. Sies H, editor. Oxidative stress: Eustress and distress. London United Kingdom, San Diego CA United States: Academic Press is an imprint of Elsevier; 2020.

9. Zhang L, Wang N-L, Zhang W, Chang Z-J. Suppression of cell proliferation by inhibitors to redox signaling in human lens epithelial cells. Zhonghua Yan Ke Za Zhi 2008; 44(7):622–8.

10. Gellert M, Venz S, Mitlöhner J, Cott C, Hanschmann E-M, Lillig CH. Identification of a dithiol-disulfide switch in collapsin response mediator protein 2 (CRMP2) that is toggled in a model of neuronal differentiation. J Biol Chem 2013; 288(49):35117–25.

11. Enoksson M, Fernandes AP, Prast S, Lillig CH, Holmgren A, Orrenius S. Overexpression of glutaredoxin 2 attenuates apoptosis by preventing cytochrome c release. Biochem Biophys Res Commun 2005; 327(3):774–9.

12. Hanschmann E-M, Godoy JR, Berndt C, Hudemann C, Lillig CH. Thioredoxins, glutaredoxins, and peroxiredoxins--molecular mechanisms and health significance: from cofactors to antioxidants to redox signaling. Antioxid Redox Signal 2013; 19(13):1539–605.

13. Miseta A, Csutora P. Relationship between the occurrence of cysteine in proteins and the complexity of organisms. Mol Biol Evol 2000; 17(8):1232–9.

14. Bräutigam L, Jensen LDE, Poschmann G, Nyström S, Bannenberg S, Dreij K et al. Glutaredoxin regulates vascular development by reversible glutathionylation of sirtuin 1. Proc Natl Acad Sci U S A 2013; 110(50):20057–62.

15. Berndt C, Lillig CH, Flohé L. Redox regulation by glutathione needs enzymes. Front Pharmacol 2014; 5:168.

16. Jones DP, Sies H. The Redox Code. Antioxid Redox Signal 2015; 23(9):734–46.

17. Santolini J, Wootton SA, Jackson AA, Feelisch M. The Redox architecture of physiological function. Curr Opin Physiol 2019; 9:34–47.

18. Prozorovski T, Schneider R, Berndt C, Hartung H-P, Aktas O. Redox-regulated fate of neural stem progenitor cells. Biochim Biophys Acta 2015; 1850(8):1543–54.

19. Holmgren A. Hydrogen donor system for Escherichia coli ribonucleoside-diphosphate reductase dependent upon glutathione. Proc Natl Acad Sci U S A 1976; 73(7):2275–9.

20. Berndt C, Lillig CH, Holmgren A. Thiol-based mechanisms of the thioredoxin and glutaredoxin systems: implications for diseases in the cardiovascular system. Am J Physiol Heart Circ Physiol 2007; 292(3):H1227-36.

21. Beer SM, Taylor ER, Brown SE, Dahm CC, Costa NJ, Runswick MJ et al. Glutaredoxin 2 catalyzes the reversible oxidation and glutathionylation of mitochondrial membrane thiol proteins: implications for mitochondrial redox regulation and antioxidant DEFENSE. J Biol Chem 2004; 279(46):47939–51.

22. Berndt C, Christ L, Rouhier N, Mühlenhoff U. Glutaredoxins with iron-sulphur clusters in eukaryotes - Structure, function and impact on disease. Biochim Biophys Acta Bioenerg 2021; 1862(1):148317.

23. Lillig CH, Berndt C, Vergnolle O, Lönn ME, Hudemann C, Bill E et al. Characterization of human glutaredoxin 2 as iron-sulfur protein: a possible role as redox sensor. Proc Natl Acad Sci U S A 2005; 102(23):8168–73.

24. Lillig CH, Berndt C. Glutaredoxins in thiol/disulfide exchange. Antioxid Redox Signal 2013; 18(13):1654–65.

25. Johansson C, Lillig CH, Holmgren A. Human mitochondrial glutaredoxin reduces S-glutathionylated proteins with high affinity accepting electrons from either glutathione or thioredoxin reductase. J Biol Chem 2004; 279(9):7537–43.

26. Wu H, Xing K, Lou MF. Glutaredoxin 2 prevents H(2)O(2)-induced cell apoptosis by protecting complex I activity in the mitochondria. Biochim Biophys Acta 2010; 1797(10):1705–15.

27. Lönn ME, Hudemann C, Berndt C, Cherkasov V, Capani F, Holmgren A et al. Expression pattern of human glutaredoxin 2 isoforms: identification and characterization of two testis/cancer cell-specific isoforms. Antioxid Redox Signal 2008; 10(3):547–57.

28. Lillig CH, Berndt C, Holmgren A. Glutaredoxin systems. Biochim Biophys Acta 2008; 1780(11):1304–17.

29. Schieber M, Chandel NS. ROS function in redox signaling and oxidative stress. Curr Biol 2014; 24(10):R453-62.

30. Liaghati A, Pileggi CA, Parmar G, Patten DA, Hadzimustafic N, Cuillerier A et al. Grx2 Regulates Skeletal Muscle Mitochondrial Structure and Autophagy. Front Physiol 2021; 12:604210.

31. Maffezzini C, Calvo-Garrido J, Wredenberg A, Freyer C. Metabolic regulation of neurodifferentiation in the adult brain. Cell Mol Life Sci 2020; 77(13):2483–96.

32. Chalker J, Gardiner D, Kuksal N, Mailloux RJ. Characterization of the impact of glutaredoxin-2 (GRX2) deficiency on superoxide/hydrogen peroxide release from cardiac and liver mitochondria. Redox Biol 2018; 15:216–27.

33. Marí M, Morales A, Colell A, García-Ruiz C, Fernández-Checa JC. Mitochondrial glutathione, a key survival antioxidant. Antioxid Redox Signal 2009; 11(11):2685–700.

34. Lisowski P, Kannan P, Mlody B, Prigione A. Mitochondria and the dynamic control of stem cell homeostasis. EMBO Rep 2018; 19(5).

35. Zhang H, Badur MG, Divakaruni AS, Parker SJ, Jäger C, Hiller K et al. Distinct Metabolic States Can Support Self-Renewal and Lipogenesis in Human Pluripotent Stem Cells under Different Culture Conditions. Cell Rep 2016; 16(6):1536–47.

36. Dahan P, Lu V, Nguyen RMT, Kennedy SAL, Teitell MA. Metabolism in pluripotency: Both driver and passenger? J Biol Chem 2019; 294(14):5420–9.

37. Sarsour EH, Kumar MG, Chaudhuri L, Kalen AL, Goswami PC. Redox control of the cell cycle in health and disease. Antioxid Redox Signal 2009; 11(12):2985–3011.

38. Lee YM, He W, Liou Y-C. The redox language in neurodegenerative diseases: oxidative post-translational modifications by hydrogen peroxide. Cell Death Dis 2021; 12(1):58.

39. Mailloux RJ, Jin X, Willmore WG. Redox regulation of mitochondrial function with emphasis on cysteine oxidation reactions. Redox Biol 2014; 2:123–39.

40. Johansson C, Kavanagh KL, Gileadi O, Oppermann U. Reversible sequestration of active site cysteines in a 2Fe-2S-bridged dimer provides a mechanism for glutaredoxin 2 regulation in human mitochondria. J Biol Chem 2007; 282(5):3077–82.

41. Scalcon V, Folda A, Lupo MG, Tonolo F, Pei N, Battisti I et al. Mitochondrial depletion of glutaredoxin 2 induces metabolic dysfunction-associated fatty liver disease in mice. Redox Biol 2022; 51:102277.

42. Zhang H, Du Y, Zhang X, Lu J, Holmgren A. Glutaredoxin 2 reduces both thioredoxin 2 and thioredoxin 1 and protects cells from apoptosis induced by auranofin and 4-hydroxynonenal. Antioxid Redox Signal 2014; 21(5):669–81.

43. Bungard D, Fuerth BJ, Zeng P-Y, Faubert B, Maas NL, Viollet B et al. Signaling kinase AMPK activates stress-promoted transcription via histone H2B phosphorylation. Science 2010; 329(5996):1201–5.

44. Wani GA, Sprenger H-G, Ndoci K, Chandragiri S, Acton RJ, Schatton D et al. Metabolic control of adult neural stem cell self-renewal by the mitochondrial protease YME1L. Cell Rep 2022; 38(7):110370.

45. Večeřa J, Procházková J, Šumberová V, Pánská V, Paculová H, Lánová MK et al. Hypoxia/Hif1α prevents premature neuronal differentiation of neural stem cells through the activation of Hes1. Stem Cell Res 2020; 45:101770.

46. Wenger RH, Gassmann M. Oxygen(es) and the hypoxia-inducible factor-1. Biol Chem 1997; 378(7):609–16.

47. Fawal M-A, Davy A. Impact of Metabolic Pathways and Epigenetics on Neural Stem Cells. Epigenet Insights 2018; 11:2516865718820946.

48. Li D, Ding Z, Gui M, Hou Y, Xie K. Metabolic Enhancement of Glycolysis and Mitochondrial Respiration Are Essential for Neuronal Differentiation. Cell Reprogram 2020; 22(6):291–9.

49. Zheng X, Boyer L, Jin M, Mertens J, Kim Y, Ma L et al. Metabolic reprogramming during neuronal differentiation from aerobic glycolysis to neuronal oxidative phosphorylation. Elife 2016; 5.

50. Martano G, Borroni EM, Lopci E, Cattaneo MG, Mattioli M, Bachi A et al. Metabolism of Stem and Progenitor Cells: Proper Methods to Answer Specific Questions. Front Mol Neurosci 2019; 12:151.

51. Bräutigam L, Schütte LD, Godoy JR, Prozorovski T, Gellert M, Hauptmann G et al. Vertebrate-specific glutaredoxin is essential for brain development. Proc Natl Acad Sci U S A 2011; 108(51):20532–7.

52. Berndt C, Poschmann G, Stühler K, Holmgren A, Bräutigam L. Zebrafish heart development is regulated via glutaredoxin 2 dependent migration and survival of neural crest cells. Redox Biol 2014; 2:673–8.

53. Gellert M, Richter E, Mostertz J, Kantz L, Masur K, Hanschmann E-M et al. The cytosolic isoform of glutaredoxin 2 promotes cell migration and invasion. Biochim Biophys Acta Gen Subj 2020; 1864(7):129599.

54. Wilms C, Lepka K, Häberlein F, Edwards S, Felsberg J, Pudelko L et al. Glutaredoxin 2 promotes SP-1-dependent CSPG4 transcription and migration of wound healing NG2 glia and glioma cells: Enzymatic Taoism. Redox Biol 2022; 49:102221.

55. Noguchi M, Kasahara A. Mitochondrial dynamics coordinate cell differentiation. Biochem Biophys Res Commun 2018; 500(1):59–64.

56. Mailloux RJ, Xuan JY, McBride S, Maharsy W, Thorn S, Holterman CE et al. Glutaredoxin-2 is required to control oxidative phosphorylation in cardiac muscle by mediating deglutathionylation reactions. J Biol Chem 2014; 289(21):14812–28.

57. Le Gal K, Schmidt EE, Sayin VI. Cellular Redox Homeostasis. Antioxidants (Basel) 2021; 10(9).

58. Guo W, Patzlaff NE, Jobe EM, Zhao X. Isolation of multipotent neural stem or progenitor cells from both the dentate gyrus and subventricular zone of a single adult mouse. Nat Protoc 2012; 7(11):2005–12.

59. Zink A, Lisowski P, Prigione A. Generation of Human iPSC-derived Neural Progenitor Cells (NPCs) as Drug Discovery Model for Neurological and Mitochondrial Disorders. Bio Protoc 2021; 11(5):e3939.

60. Richter-Landsberg C, Heinrich M. OLN-93: A new permanent oligodendroglia cell line derived from primary rat brain glial cultures. J. Neurosci. Res. 1996; 45(2):161–73.

61. Son JH, Chun HS, Joh TH, Cho S, Conti B, Lee JW. Neuroprotection and Neuronal Differentiation Studies Using Substantia Nigra Dopaminergic Cells Derived from Transgenic Mouse Embryos. J. Neurosci. 1999; 19(1):10–20.

62. Ippolito DM, Eroglu C. Quantifying synapses: an immunocytochemistry-based assay to quantify synapse number. J Vis Exp 2010; (45).

63. SDS-PAGE Gel. Cold Spring Harb Protoc 2015; 2015(7):pdb.rec087908.

64. Martínez M, Martínez NA, Silva WI. Measurement of the Intracellular Calcium Concentration with Fura-2 AM Using a Fluorescence Plate Reader. Bio Protoc 2017; 7(14):e2411.

65. Malgaroli A, Milani D, Meldolesi J, Pozzan T. Fura-2 measurement of cytosolic free Ca2+ in monolayers and suspensions of various types of animal cells. J Cell Biol 1987; 105(5):2145–55.

66. Habich M, Riemer J. Detection of Cysteine Redox States in Mitochondrial Proteins in Intact Mammalian Cells. Methods Mol Biol 2017; 1567:105–38.

67. Pasterkamp RJ. Getting neural circuits into shape with semaphorins. Nat Rev Neurosci 2012; 13(9):605–18.

68. Fernández-Gamba A, Leal MC, Maarouf CL, Richter-Landsberg C, Wu T, Morelli L et al. Collapsin response mediator protein-2 phosphorylation promotes the reversible retraction of oligodendrocyte processes in response to non-lethal oxidative stress. J Neurochem 2012; 121(6):985–95.

69. Ono K, Hirahara Y, Gotoh H, Nomura T, Takebayashi H, Yamada H et al. Origin of Oligodendrocytes in the Vertebrate Optic Nerve: A Review. Neurochem Res 2018; 43(1):3–11.

70. Lee Y-X, Lin P-H, Rahmawati E, Ma Y-Y, Chan C, Tzeng C-R. Mitochondria Research in Human Reproduction. In: The Ovary. Elsevier; 2019. p. 327–35.

71. Zorova LD, Popkov VA, Plotnikov EY, Silachev DN, Pevzner IB, Jankauskas SS et al. Mitochondrial membrane potential. Anal Biochem 2018; 552:50–9.

72. Gut P, Verdin E. The nexus of chromatin regulation and intermediary metabolism. Nature 2013; 502(7472):489–98.

73. Meyer N, Rinholm JE. Mitochondria in Myelinating Oligodendrocytes: Slow and Out of Breath? Metabolites 2021; 11(6).

74. Estrin GL, Bhavnani S. Brain Development: Structure. In: Benson JB, editor. Encyclopedia of Infant and Early Childhood Development. 2nd ed. San Diego: Elsevier; 2020. p. 205–14.

75. Ziak J, Weissova R, Jeřábková K, Janikova M, Maimon R, Petrasek T et al. CRMP2 mediates Sema3F-dependent axon pruning and dendritic spine remodeling. EMBO Rep 2020; 21(3):e48512.

76. Stratton H, Boinon L, Moutal A, Khanna R. Coordinating Synaptic Signaling with CRMP2. Int J Biochem Cell Biol 2020; 124:105759.

77. Brustovetsky T, Khanna R, Brustovetsky N. Involvement of CRMP2 in Regulation of Mitochondrial Morphology and Motility in Huntington's Disease. Cells 2021; 10(11).

78. Quartu M, Serra MP, Boi M, Ibba V, Melis T, Del Fiacco M. Polysialylated-neural cell adhesion molecule (PSA-NCAM) in the human trigeminal ganglion and brainstem at prenatal and adult ages. BMC Neurosci 2008; 9:108.

79. Ho S-Y, Chao C-Y, Huang H-L, Chiu T-W, Charoenkwan P, Hwang E. NeurphologyJ: an automatic neuronal morphology quantification method and its application in pharmacological discovery. BMC Bioinformatics 2011; 12:230.

80. Komiya Y, Habas R. Wnt signal transduction pathways. Organogenesis 2008; 4(2):68–75.

81. Arenas E. Wnt signaling in midbrain dopaminergic neuron development and regenerative medicine for Parkinson's disease. J Mol Cell Biol 2014; 6(1):42–53.

82. Sousa KM, Villaescusa JC, Cajanek L, Ondr JK, Castelo-Branco G, Hofstra W et al. Wnt2 regulates progenitor proliferation in the developing ventral midbrain. J Biol Chem 2010; 285(10):7246–53.

83. Chatterjee S, Sil PC. ROS-Influenced Regulatory Cross-Talk With Wnt Signaling Pathway During Perinatal Development. Front Mol Biosci 2022; 9:889719.

84. Ribeiro D, Ellwanger K, Glagow D, Theofilopoulos S, Corsini NS, Martin-Villalba A et al. Dkk1 regulates ventral midbrain dopaminergic differentiation and morphogenesis. PLoS One 2011; 6(2):e15786.

85. Fazel Darbandi S, Robinson Schwartz SE, Pai EL-L, Everitt A, Turner ML, Cheyette BNR et al. Enhancing WNT Signaling Restores Cortical Neuronal Spine Maturation and Synaptogenesis in Tbr1 Mutants. Cell Rep 2020; 31(2):107495.

86. Li F, Tsien JZ. Memory and the NMDA receptors. N Engl J Med 2009; 361(3):302–3.

87. Saab AS, Tzvetavona ID, Trevisiol A, Baltan S, Dibaj P, Kusch K et al. Oligodendroglial NMDA Receptors Regulate Glucose Import and Axonal Energy Metabolism. Neuron 2016; 91(1):119–32.

88. Krasnow AM, Attwell D. NMDA Receptors: Power Switches for Oligodendrocytes. Neuron 2016; 91(1):3–5.

89. Káradóttir R, Cavelier P, Bergersen LH, Attwell D. NMDA receptors are expressed in oligodendrocytes and activated in ischaemia. Nature 2005; 438(7071):1162–6.

90. Janáky R, Ogita K, Pasqualotto BA, Bains JS, Oja SS, Yoneda Y et al. Glutathione and signal transduction in the mammalian CNS. J Neurochem 1999; 73(3):889–902.

91. Cummings KA, Popescu GK. Glycine-dependent activation of NMDA receptors. J Gen Physiol 2015; 145(6):513–27.

92. Brennan AM, Suh SW, Won SJ, Narasimhan P, Kauppinen TM, Lee H et al. NADPH oxidase is the primary source of superoxide induced by NMDA receptor activation. Nat Neurosci 2009; 12(7):857–63.

93. Johnson-Cadwell LI, Jekabsons MB, Wang A, Polster BM, Nicholls DG. 'Mild Uncoupling' does not decrease mitochondrial superoxide levels in cultured cerebellar granule neurons but decreases spare respiratory capacity and increases toxicity to glutamate and oxidative stress. J Neurochem 2007; 101(6):1619–31.

94. MacDonald JF, Jackson MF, Beazely MA. Hippocampal long-term synaptic plasticity and signal amplification of NMDA receptors. Crit Rev Neurobiol 2006; 18(1-2):71–84.

95. Masutani H, Bai J, Kim Y-C, Yodoi J. Thioredoxin as a neurotrophic cofactor and an important regulator of neuroprotection. Mol Neurobiol 2004; 29(3):229–42.

96. Tian L, Nie H, Zhang Y, Chen Y, Peng Z, Cai M et al. Recombinant human thioredoxin-1 promotes neurogenesis and facilitates cognitive recovery following cerebral ischemia in mice. Neuropharmacology 2014; 77:453–64.

97. Iqbal MA, Eftekharpour E. Regulatory Role of Redox Balance in Determination of Neural Precursor Cell Fate. Stem Cells Int 2017; 2017.

98. Dincman TA, Beare JE, Ohri SS, Whittemore SR. Isolation of cortical mouse oligodendrocyte precursor cells. J Neurosci Methods 2012; 209(1):219–26.

99. Azzarelli R, Oleari R, Lettieri A, Andre' V, Cariboni A. In Vitro, Ex Vivo and In Vivo Techniques to Study Neuronal Migration in the Developing Cerebral Cortex. Brain Sci 2017; 7(5).

100. Malinow R, Hayashi Y, Maletic-Savatic M, Zaman SH, Poncer J-C, Shi S-H et al. Introduction of green fluorescent protein (GFP) into hippocampal neurons through viral infection. Cold Spring Harb Protoc 2010; 2010(4):pdb.prot5406.

101. Schoenfeld R, Wong A, Silva J, Li M, Itoh A, Horiuchi M et al. Oligodendroglial differentiation induces mitochondrial genes and inhibition of mitochondrial function represses oligodendroglial differentiation. Mitochondrion 2009; 10(2):143–50.

102. Akanji MA, Rotimi DE, Elebiyo TC, Awakan OJ, Adeyemi OS. Redox Homeostasis and Prospects for Therapeutic Targeting in Neurodegenerative Disorders. Oxid Med Cell Longev 2021; 2021:9971885.

103. Nishimura T, Fukata Y, Kato K, Yamaguchi T, Matsuura Y, Kamiguchi H et al. CRMP-2 regulates polarized Numb-mediated endocytosis for axon growth. Nat Cell Biol 2003; 5(9):819–26.

104. Schmidt EF, Strittmatter SM. The CRMP family of proteins and their role in Sema3A signaling. Adv Exp Med Biol 2007; 600:1–11.

105. Khanna R, Moutal A, Perez-Miller S, Chefdeville A, Boinon L, Patek M. Druggability of CRMP2 for Neurodegenerative Diseases. ACS Chem Neurosci 2020; 11(17):2492–505.

106. Papadia S, Soriano FX, Léveillé F, Martel M-A, Dakin KA, Hansen HH et al. Synaptic NMDA receptor activity boosts intrinsic antioxidant defenses. Nat Neurosci 2008; 11(4):476–87.

107. Choi YB, Lipton SA. Redox modulation of the NMDA receptor. Cell Mol Life Sci 2000; 57(11):1535–41.

108. Choi Y-B, Chen H-SV, Lipton SA. Three Pairs of Cysteine Residues Mediate Both Redox and Zn2+ Modulation of the NMDA Receptor. J Neurosci 2001; 21(2):392–400.

109. Levy DI, Sucher NJ, Lipton SA. Glutathione prevents N-methyl-D-aspartate receptor-mediated neurotoxicity. Neuroreport 1991; 2(6):345–7.

110. Janáky R, Varga V, Saransaari P, Oja SS. Glutathione modulates the N-methyl-D-aspartate receptor-activated calcium influx into cultured rat cerebellar granule cells. Neurosci Lett 1993; 156(1-2):153–7.

10. List of Abbreviations

ATP	adenosine triphosphate
AMP	adenosine monophosphate
CRMP2	collapsin response mediator protein 2
Dkk1	Dickkopf related protein 1
DNA	deoxyribonucleotide
DNMT	DNA methyltransferase
ETC	electron transfer chain
GSH	glutathione
GSSG	glutathione disulfide
GR	glutathione reductase
H2O2	hydrogen peroxide
Hif-1	hypoxia inducible factor 1
HMT	Methyltransferase
iPSC	induced pluripotent stem cells
KO	knock out
MBP	myelin binding protein
MMP	mitochondrial membrane potential
mmPEG	methoxypolyethylene glycol chain substituted maleimide probe
NADPH	nicotinamide adenine dinucleotide phosphate
NEM	N-ethylmaleimide
NG2	chondroitin sulfate proteoglycan nerve/glial antigen 2
NMDAR	N-methyl-D-aspartate receptors
NRF2	nuclear factor erythroid 2-related factor 2
NSC	neural stem cell
olig 2	oligodendrocyte lineage factor 2
OPC	oligodendrocyte precursor cell
OXPHOS	oxidative phosphorylation
Prx	peroxiredoxins
ROS	reactive oxygen species
SGZ	sub granular zone
SOD	superoxide dismutase
SVZ	subventricular zone
TCA	tricarboxylic cycle
TCEP	Tris(2-chlorethyl)phosphate
Trx	thioredoxin